SLAC-PUB-7133
April, 1996

# The Experimental Investigation of Supersymmetry Breaking

MICHAEL E. PESKIN*
*Stanford Linear Accelerator Center*
*Stanford University, Stanford, California 94309 USA*

ABSTRACT

If Nature is supersymmetric at the weak interaction scale, what can we hope to learn from experiments on supersymmetric particles? The most mysterious aspect of phenomenological supersymmetry is the mechanism of spontaneous supersymmetry breaking. This mechanism ties the observable pattern of supersymmetric particle masses to aspects of the underlying unified theory at very small distance scales. In this article, I will discuss a systematic experimental program to determine the mechanism of supersymmetry breaking. Both $pp$ and $e^+e^-$ colliders of the next generation play an essential role.

to appear in the proceedings of the Yukawa International Seminar (YKIS-95)
Kyoto, Japan, August 21-25, 1995

* Work supported by the Department of Energy, contract DE–AC03–76SF00515.

# The Experimental Investigation of Supersymmetry Breaking

Michael E. PESKIN*

*Stanford Linear Accelerator Center, Stanford University*
*Stanford, California 94309 USA*

(Received April 16, 1996 )

If Nature is supersymmetric at the weak interaction scale, what can we hope to learn from experiments on supersymmetric particles? The most mysterious aspect of phenomenological supersymmetry is the mechanism of spontaneous supersymmetry breaking. This mechanism ties the observable pattern of supersymmetric particle masses to aspects of the underlying unified theory at very small distance scales. In this article, I will discuss a systematic experimental program to determine the mechanism of supersymmetry breaking. Both $pp$ and $e^+e^-$ colliders of the next generation play an essential role.

## §1. Introduction

Today, many theorists and experimenters expect that, on energy scales that will soon be probed by accelerators, Nature is supersymmetric, symmetric between fermions and bosons in the spectrum of fundamental particles. Part of the motivation for this idea comes from experiment. The assumption of supersymmetry allows the values of the standard model gauge couplings, now precisely measured at LEP and other facilities, to be consistent with grand unification, and it allows the observed large value of the top quark mass to lead naturally to electroweak symmetry breaking. Reviews of these two ideas can be found, respectively, in Refs. 1, 2; more general reviews of phenomenological supersymmetry are given in Refs. 3 and 4, and 5. However, the most compelling arguments for supersymmetry come from its seductive mathematical beauty and its deep connection to string theory and other theories of quantum gravity.

The mathematical motivations for supersymmetry lead to research programs that have very little direct contact with experiment, for example, investigations of the invariance groups of supersymmetric theories near the Planck scale, of compactification of higher dimensions, and of the nonperturbative, Planck-energy, spectrum. The intense interest in these topics has led many people to wonder if the directions of phenomenological and mathematical research in elementary particle physics have split permanently, so that they can never be rejoined by future developments.

Certainly, the current experimental situation offers little evidence that these lines will eventually connect. This will remain true as long as mathematical theory insists that the most important feature of physics at the TeV energy scale is that it is supersymmetric, while experiment sees no direct evidence for physics outside the standard model. But I often hear much stronger doubts expressed. Some of my theoretical colleagues argue that, even in the future, even if compelling evidence for supersymmetry is discovered, experiment might not have enough to say that is truly of interest to people making deep mathematical investigations. And my experimental colleagues have been arguing for years that the physics of Planck energies and higher dimensions is so far

* E-mail address: mpeskin@slac.stanford.edu

removed from the experimentally accessible domain that it is difficult to conceive of any experimental result that would alter or reorient this theoretical program.

Personally, I am much more optimistic. Though I am thoroughly seduced by the beauty of superstring theory, I recognize that supersymmetry might not be preserved down to the TeV scale. However, it is reasonable to accept this as a working hypothesis, if only because this provides a needed mechanism for electroweak symmetry breaking. Under this hypothesis, we should find supersymmetric particles either at the current generation of accelerators or at the next step, and I intend to keep the faith until a thorough search is made. But to answer the questions raised in the previous paragraph, it is necessary to think through carefully to the next step of the experimental program that will follow this discovery. Once supersymmetric particles are found, what can we learn about them? In particular, can we use them to gain insight into the truly fundamental issues in Nature which are fully revealed only at the unification or superstring mass scale? I believe that the answer to this questions is yes, and in this paper I will explain how it can be done.

Though the grand question of how we imagine the connection of theory and experiment is a major issue for our field, and is itself a motivation to analyze this problem in advance of the discovery of supersymmetry, there is another pressing motivation as well. Experimental high-energy physics cannot exist without accelerators, and as accelerators become more complex and expensive, we must be sure that we request the correct ones for the task at hand. The time scale for the construction of accelerators is of the order of a decade, and in the US we have learned painfully that the process may conclude with our government's insistence that we scrap everything and start over from the beginning. Thus, it is important that we think clearly about the physics goals of experiments that will be conducted a decade from now. For many of the options for the physics of the TeV energy scale, it is very difficult to see ahead so far. But the special properties of supersymmetric theory—the fact that it connects naturally to fundamental theories at very high energy and also the fact that it involves only weak-coupling interactions at the TeV scale—allow us to look quite far down the road that we will have to travel experimentally if this hypothesis is realized. Supersymmetry thus gives us a concrete example of what the experimental physics of the year 2005 could look like, and we can use the detailed picture that it provides to draw conclusions about the accelerator facilities we will need in that era. We must of course keep in mind that we do not know what theory of TeV physics Nature actually chooses, so that supersymmetry should be only one of many possibilities we must survey. Here, I will only discuss the case of supersymmetry. A broader survey of models of electroweak symmetry breaking, which reaches the same general conclusion within a larger set of models, is given in Ref. 6.

The plan of this paper is as follows: In Section 2, I will discuss the most important open question in supersymmetry phenomenology, that of the mechanism of supersymmetry breaking. I will review the general constraints on the nature of supersymmetry breaking and the various models of this phenomenon which have been proposed in the literature. In Section 3, I will present a three-step experimental program to distinguish the various models discussed in Section 2 and thus resolve experimentally the origin of supersymmetry breaking. In Section 4, I will discuss the contributions to this program which can be expected from $pp$ colliders, and, in particular, from the LHC. In

Section 5, I will discuss the contributions to this program which can be supplied by $e^+e^-$ linear colliders of the next generation, and I will demonstrate the essential role that $e^+e^-$ experiments will play in this investigation. Section 6 will give some general conclusions.

## §2. Phenomenological Theory of Supersymmetry Breaking

In this paper, I will assume that Nature is supersymmetric at the weak interaction scale, and that ingredients of the supersymmetric theory provide the mechanism of electroweak symmetry breaking. This hypothesis can be used to place upper limits on the masses of supersymmetric particles. If supersymmetry is the mechanism of electroweak symmetry breaking, the $W$ and $Z$ masses are directly related to the mass scale of supersymmetry. The exact correspondence between the $Z$ mass and the mass of, say, the supersymmetry partners of the electron is model-dependent. However, the ratio between these masses cannot be made arbitrarily large without a fine adjustment of parameters. Several groups have tried to characterize the reasonable range of allowable fine tuning and to convert this range to a set of bounds on particle masses.[7] The most characteristic of these are limits on the masses of the $W$ and gluon partners,

$$m(\tilde{w}) < 250\text{GeV} , \qquad m(\tilde{g}) < 800\text{GeV} . \tag{2·1}$$

These limits imply that supersymmetric partners should be found, at the latest, at the LHC and at the next generation of $e^+e^-$ colliders.

In my analysis here, I will assume that the first signals of supersymmetry have been found, and I will be concerned with the questions at the next level to be explored. When I discuss the results of specific experiments, I will make one further assumption, that there is a conserved 'R-parity' which makes the lightest supersymmetric partner stable. Then supersymmetric particle production will be characterized by signatures of missing energy and unbalanced momentum which should be visible both at lepton and at hadron colliders. If supersymmetric particles are present but R-parity is violated, there should be a similarly rich program involving signatures with lepton or baryon number violation; see, for example, Refs. 4 and 8.

Assuming, then, that supersymmetric partners are found, what is the next question that we would like to answer? A simple reply is that we will want to measure the masses of these supersymmetric partners and understand their properties systematically. I will address this issue in more detail.

The equation of motion of a supersymmetric extension of the standard model has three parts. Of these, two are highly constrained by supersymmetry: The gauge interactions of superpartners are fixed by their $SU(3)\times SU(2)\times U(1)$ quantum numbers, and the renormalizable couplings of quark, lepton, and Higgs partners are fixed to be equal to the corresponding couplings of the standard model. However, the third piece of the puzzle is a complete mystery. If we wish to understand why the partners of quarks and leptons are heavy, we must appeal to some mechanism of spontaneous supersymmetry breaking. This mechanism is unknown and is not constrained by a direct connection to any known physics. This mechanism controls the regularities of the supersymmetric mass spectrum and the possible mixings between superpartner states. It also controls the other important qualitative features of the theory. For example, the various sources

of the Higgs boson masses which lead eventually to $SU(2)\times U(1)$ breaking have their origin in supersymmetry breaking.

Supersymmetry breaking also connects the phenomenology of supersymmetry to the truly deep questions about the structure of elementary particles. If Nature is supersymmetric and weakly-coupled at the TeV scale, it is reasonable that the strong, weak, and electromagnetic interactions are grand-unified at very high energy. We already have some information about this unification from the values of the gauge couplings, and from the ratio $m_b/m_\tau$. From a first point of view, the measurement of supersymmetry breaking will give us access to a new set of parameters, outside those which are directly connected to the standard model couplings, from which we can obtain new pieces of evidence on the properties of the unified theory. But there is also a more ambitious point view. In models in which one attempts to derive the whole structure of Nature from a superstring model, supersymmetry breaking typically arises from sectors of the theory which have an essential connection to the string origins of the model, for example, from the interactions of the 'dilaton' and 'moduli' fields and the gauge fields of 'hidden' sectors,[9,10] or from the transmutation of dimensions that occurs in string theory at strong coupling.[11] If we can study the pattern of supersymmetry breaking experiment ally, we might obtain a direct window into these deep structures.

### *2.1. Issues of supersymmetry breaking*

What, exactly, do we wish to know about supersymmetry breaking? At the first level of any discussion of the physics of supersymmetry breaking, two questions arise. The answers to these questions would take us a long way toward an understanding of supersymmetry breaking and its relation to the other fundamental interactions.

The first of these questions is the mass scale of supersymmetry breaking and, as a closely connected issue, the scale of the transmission of supersymmetry breaking. The interplay of these scales deserves some explanation. To begin, we should recall why it is that the quarks and leptons are expected to be lighter than their superpartners, rather than the other way around. Quarks and leptons can receive mass only if $SU(2)\times U(1)$ is spontaneously broken. However, their partners—squarks and sleptons—are scalars, and there is no principle of quantum field theory that prohibits scalar fields from obtaining a mass. What keeps the quark and lepton partners light is their supersymmetry relation to their fermion partners. If supersymmetry is spontaneously broken in some sector of Nature, and this sector communicates with the quarks and leptons and their partners through some interactions, the supersymmetry breaking will be transmitted to the squarks and sleptons to produce scalar masses and other soft interactions. Call the scale of these masses $m_S$. The Higgs boson masses will also be of scale $m_S$. The Higgs vacuum expectation value will also be of size $m_S$, up to coupling constants, and so $m_S$ will determine the location of the weak interaction scale. Then, finally, masses are fed down to the quarks and leptons according to the strength of their coupling to the Higgs sector.

The value of $m_S$ is determined by the underlying physics responsible for spontaneous supersymmetry breaking. Let $\Lambda$ be the mass scale of spontaneous supersymmetry breaking, and let $M$ be the mass of the particles that connect the symmetry-breaking sector to the quarks, leptons, and standard model gauge bosons. I will refer to $M$ as the 'messenger scale', and it will play a crucial role in our analysis. Though the relation

between $M$, $\Lambda$, and $m_S$ is model-dependent, the general form of this relation is given by the equation

$$m_S \sim \frac{\Lambda^2}{M} , \tag{2·2}$$

so that different choices for $\Lambda$ and $M$ are correlated by the fact that they must generate $m_S \sim m_Z$.

By default, gravity (or supergravity) is the messenger. This was made clear in the beautiful foundational papers of Cremmer and collaborators,[12] who showed explicitly how supersymmetry breaking is transferred from the original symmetry-breaking sector to the rest of Nature through supergravity interactions. More generally, the messenger interactions might be associated with the grand unified scale or other flavor physics, with some intermediate scale, or with the standard model gauge interactions. The nature of the messenger plays an important role in determining the form and selection rules for the supersymmetry breaking masses and interactions.

If this were our only information about $M$ and $\Lambda$, there would be considerable room for speculation. Fortunately, the range of possible theories that lead to $M$ and $\Lambda$ is limited by additional constraints. These stem from the second problem that the mechanism of supersymmetry breaking must solve, the 'supersymmetric flavor problem'. To understand this issue, let us write the formula for the mass matrix of the scalar partners of the $d$, $s$, $b$ quarks. Since in supersymmetry left- and right-handed fermions have independent complex scalar fields as their superpartners, I will write this matrix as a $2 \times 2$ matrix of $3 \times 3$ blocks, acting on a vector

$$\begin{pmatrix} \tilde{d}_L^i \\ \tilde{d}_R^i \end{pmatrix} \tag{2·3}$$

where $i$ is the generation label, $i = 1, 2, 3$. The mass matrix gets contributions from four sources, two of which are supersymmetric—the quark mass matrix $m_d$ of the standard model, and the combination of this term with the Higgs mass parameter $\mu$—and two of which arise from supersymmetry-breaking—scalar field mass matrices $m_{dL}^2$ and $m_{dR}^2$, and a mixing term generated by a supersymmetry-breaking 3-scalar term involving the Higgs field. The final result is a matrix

$$\mathcal{M}^2 = \begin{pmatrix} m_{dL}^2 + m_d m_d^\dagger & -m_d(A + \mu \tan\beta) \\ -m_d^\dagger(A + \mu \tan\beta) & m_{dR}^2 + m_d^\dagger m_d \end{pmatrix} . \tag{2·4}$$

In this equation, $\tan\beta$ is the ratio of the two Higgs field vacuum expectation values required in the minimal supersymmetric extension of the standard model: $\tan\beta = < h_2^0 > / < h_1^0 > = v_2/v_1$. This parameter infects all of supersymmetry phenomenology. I have simplified the expression by writing the 3-scalar term in terms of a constant parameter $A$. In principle, this could also be a matrix with flavor indices.

The quark mass matrix $m_d$ is not intrinsically diagonal. In standard weak interaction phenomenology, we diagonalized it with matrices $V_L$ and $V_R$ which eventually become ingredients of the Cabbibo-Kobayashi-Maskawa mixing matrix:

$$m_d = V_L^\dagger \begin{pmatrix} m_d & & \\ & m_s & \\ & & m_b \end{pmatrix} V_R . \tag{2·5}$$

Then the $Z^0$ couplings are automatically flavor-diagonal; flavor-changing neutral current effects appear only in loop diagrams, and only proportional to products of quark mass differences. This lead to the observed suppression of flavor-changing neutral current processes. However, the mass matrix (2·4) contains new sources of flavor violation through the supersymmetry-breaking scalar mass matrices $m_{dL}^2, m_{dR}^2$. Unless the diagonalization of $m_d$ also diagonalized these matrices, diagrams with supersymmetric particles in loops can provide new and dangerous sources of flavor violation. For example, applying this logic to the contribution to the $K_L$–$K_S$ mass difference due to gluino exchange, Gabbiani and Masiero[13] have derived the bound

$$\frac{(V_R m_{dR}^2 V_R^\dagger)_{12}}{m_{\tilde{d}}^2} < 10^{-2} \left(\frac{m_{\tilde{d}}}{300\ \mathrm{GeV}}\right)^2 . \qquad (2\cdot6)$$

Similar bounds on the flavor violation of the supersymmetry-breaking mass terms have been discussed by many authors.*)

*2.2. Models of supersymmetry breaking*

Why should the supersymmetry-breaking scalar masses be diagonal in the same basis as the standard model mass terms? There are a large number of explanations for this in the literature. These explanations divide into general classes which express the range of possibilities for the underlying physics of supersymmetry breaking. On the one hand, it is possible that the supersymmetry breaking scalar masses are universal among generations, so that the mass matrices $m_{dL}^2, m_{dR}^2$ are proportional to 1 and thus diagonal in any basis. Or these mass matrices may have structure, but they might also have a reason to be diagonal in the basis set by the mass matrix. On the other hand, the mechanism for the specific form of these matrices might be predetermined by the short-distance physics, or it might arise as the result of dynamical effects on larger scales. Thus, we have four classes of models:

1. **Preset Universality.** This is the original schema for supersymmetry model building which was proposed in the early papers of Dimopoulos and Georgi[15] and Sakai.[16] It is realized elegantly, with $M$ equal to the Planck mass $m_{\mathrm{Pl}}$, in models in which supersymmetry is broken at a high scale and the breaking is communicated by supergravity.[17] Other agents which couple universally to quarks and leptons can also give models of this structure.
2. **Dynamical Universality.** This class encompasses a broad range of models in which the supersymmetry-breaking mass matrices are fixed in a manner determined only by the standard model gauge couplings of superpartners. It includes the 'no-scale' models in which $m_L^2, m_R^2$ are zero at the fundamental scale and are generated by radiative corrections,[18] a model of Lanzagorta and Ross[19] in which $m_L^2, m_R^2$ are determined by an infrared fixed point, and models studied by Dine, Nelson, Nir, and Shirman[20] in which supersymmetry is broken at a low scale and communicated through the standard model gauge interactions.
3. **Preset Alignment.** This class of models attempts to build up the supersymmetry breaking mass matrices using the same principles that one uses to construct the standard model quark mass matrices (for example, the successive breaking of

*) See, for example, Ref. 3; some recent articles are given in Ref. 14.

discrete symmetries). Then these symmetry principles can insure that the two sets of matrices are diagonal in the same basis, without flavor-degeneracy of scalar masses.[21] In this class of models, it is natural for the messenger scale to be of the order of the grand unification scale.

4. **Dynamical Alignment.** In this class of models, the relative orientation of the supersymmetry-breaking and standard model mass matrices is a free parameter in the underlying theory and is determined to be aligned by radiative corrections. The one current example of a model in this class has $M$ near the Planck scale,[22], leading to a phenomenology very similar to that of the class just above. A very low value of $M$ might be more natural in this scheme and may lead to some different options.

Here are four broad classes of possibilities for the mechanism of supersymmetry breaking. It is interesting to lay out the various possibilities in this way, because it makes clear that every specific solution to the supersymmetric flavor problem entails a choice of $M$ and therefore of $\Lambda$. If we can recognize experimentally which possibility Nature chooses, we can also infer the nature of the messenger and perhaps the specific origin of supersymmetry breaking.

## §3. An Experimental Program

How can we decide which mechanism is chosen? At a certain level, it is obvious that the answer can be found by measuring the spectrum of superparticle masses. To probe more deeply, we should ask which of these measurements are easy and which are very challenging, and whether the measurements that are reasonably straightforward can actually give us the information we are looking for.

To understand how we will learn about these fundamental issues from measurements, it is necessary to work out the correspondence between properties of the supersymmetry spectrum and the various hypotheses described above. I will describe that correspondence in Section 3.3. To prepare the way, we must first discuss two issues that provide the baseline for that analysis, the masses of the gauge boson superpartners and the value of the Higgs sector parameter $\tan\beta$.

### *3.1. Gaugino masses*

In the discussion of the previous section, we concentrated our attention on the masses of the scalar partners of the quarks and leptons. The masses of the fermionic partners of gauge bosons—gauginos—did not seem to play an important role. But in fact, a precise understanding of gauginos is a prerequisite to any detailed exploration of supersymmetry. This is true for two reasons. First, gaugino masses influence scalar masses through radiative corrections. Second, the nature of the gaugino mass matrix affects the general phenomenology of supersymmetry, as viewed by collider experiments. In this section, I will review both of these issues.

The systematic of gaugino masses forms an essential part of the scalar mass problem due to the diagram shown in Fig. 1. The scalar masses are renormalized, as shown, by the transition to a gaugino and a quark or lepton. This process gives a correction

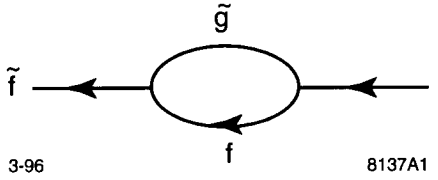


Fig. 1. Feed-down of gaugino masses into scalar masses.

to the mass which is described by the renormalization group equation

$$-\frac{dm_f^2}{d\log Q} = \sum_i \frac{2}{\pi} C_i \alpha_i m_i^2 \ , \tag{3·7}$$

where $m_f^2$ are the scalar masses and $m_i$ are the gaugino mass parameters generated by supersymmetry breaking. The coupling constants $\alpha_i$ are the standard model couplings, evaluated at the weak interaction scale, normalized as in grand unification: $\alpha_3 = \alpha_s$, $\alpha_2 = \alpha_w, \alpha_1 = (5/3)\ \alpha'$. The $C_i$ are Casimir coefficients:

$$C_1 = \frac{3}{5} Y^2 \ , \qquad C_2 = \begin{cases} \frac{3}{4} & \mathrm{L} \\ 0 & \mathrm{R} \end{cases} \ , \qquad C_3 = \begin{cases} 0 & \ell \\ \frac{4}{3} & \mathrm{q} \end{cases} \ . \tag{3·8}$$

The renormalization group equation must be integrated from the messenger scale $M$ to the weak scale. One of the ways we can determine the value of the messenger scale is to estimate how far this renormalization group equation has been evolved in order to produce the observed spectrum of scalar masses. To do that, we require the values of the gaugino masses, to set the overall scale of this effect.

At the same time that they renormalize the scalar masses, the gaugino masses evolve by their own renormalization. This means that a simple spectrum of gauginos at one scale will acquire structure as we move to a different scale. The simplest possible picture of gaugino masses is that they are grand-unified, that is, they are all equal at the grand unification scale. From this starting point, the one-loop renormalization group equation gives an interesting pattern at lower scales: The gaugino masses evolve so as to remain proportional to the gauge couplings:

$$\frac{m_1}{\alpha_1} = \frac{m_2}{\alpha_2} = \frac{m_3}{\alpha_3} \ . \tag{3·9}$$

I will refer to this systematic relation as 'gaugino unification'. The simple relation is corrected by the two-loop terms in the renormalization group equations and by finite one-loop corrections at the weak scale.[23] The only large correction comes in the finite contributions which relate the short-distance gluino mass to the physical gluino mass,[24] a problem reminiscent of the problems of the quark mass definition in QCD.

It is interesting to ask how broad a class of models obey gaugino unification. Obviously, if there is no grand unification, there is no reason for this relation to be true. However, one of the phenomenological virtues of supersymmetry is that it allows the grand unification of couplings, and so it is reasonable to assume this in model-building. Still, grand unification does not necessarily imply gaugino unification. On one hand, the messenger scale might be well below the grand unification scale, so that the physics

of gaugino mass generation is not grand unified. On the other hand, it is possible that the field which breaks supersymmetry is not a singlet of the grand unification group. A violation of gaugino universality would be a signal of one of these mechanisms and thus would be of great experimental importance. Curiously, though, the simplest models of each type actually respect the relation (3·9). For example, in the model of Ref. 20, supersymmetry is communicated from a unique standard model singlet field to a vectorlike multiplet of fields and from there though standard model gauge interactions to the partners of gauge bosons. The messenger scale is well below the grand unification scale, but the vectorlike multiplet must be a complete $SU(5)$ representation (*e.g.*, $(5 + \bar{5})$) so as not to spoil the unification relation of the low energy gauge couplings. These assumptions imply that the gaugino masses are related by (3·9). Similarly, if supersymmetry breaking is communicated at the grand unification or scale, the communication of supersymmetry breaking by an $SU(5)$-nonsinglet field involves a nonrenormalizable interaction or a perturbative correction and thus would be suppressed with respect to any nonzero contribution from singlet fields.[25)]

The experimental measurement of the gaugino mass parameters $m_i$ brings in some additional issues which we might call problems of supersymmetry engineering. These are not problems of principle, but they must be resolved to understand the deeper aspects of supersymmetry phenomenology.

The parameter $m_3$ is the only contribution to the mass of the supersymmetry partner of the gluon, the gluino, up to the usual problems of defining the mass of a colored particle. I will discuss techniques for the measurement of the gluino mass in Section 4. For the supersymmetry partners of *W*, *Z*, and $\gamma$, however, there are additional effect that contribute to their masses. Even in a supersymmetric situation, the partners of *W* and *Z* will obtain mass from the Higgs mechanism. This mass term couples the fermionic partners of the vector bosons to the fermionic partners of the Higgs bosons. These latter particles can obtain mass also from a supersymmetric mass term $\mu$, and we know from the non-observation of light superpartners at the $Z^0$ that $\mu$ is nonzero.*)

These effects are summarized as a mixing problem involving the vector boson and Higgs boson superpartners. Supersymmetric models necessarily include two Higgs doublets $h_1, h_2$; therefore, they contain physical charged Higgs fields, which have fermionic partners. Denote the left-handed fermion partners of $W^+$ and $h_2^+$ by $\tilde{w}^+, \tilde{h}_2^+$, and adopt a similar notation for the left-handed fermion partners of $W^-$ and $h_1^-$. Then the charged fermionic superparticles have a mass matrix, including all three of the effects descibed in the previous paragraph, which takes the form

$$(-i\tilde{w}^- \quad \tilde{h}_1^-) \begin{pmatrix} m_2 & \sqrt{2} m_W \sin\beta \\ \sqrt{2} m_W \cos\beta & \mu \end{pmatrix} \begin{pmatrix} -i\tilde{w}^+ \\ \tilde{h}_2^+ \end{pmatrix} . \tag{3·10}$$

This mass matrix is asymmetric, and its diagonalization will generally require a different mixing angle for the positively and negatively charged left-handed fermions. In a similar way, the partners of the *Z*, photon, and neutral Higgs bosons have a $4 \times 4$ mixing

*) A tiny corner of parameter space is still available; see Ref. 26.

problem:

$$\begin{pmatrix} m_1 & 0 & -m_Z \sin\theta_w \cos\beta & m_Z \sin\theta_w \sin\beta \\ 0 & m_2 & m_Z \cos\theta_w \cos\beta & -m_Z \cos\theta_w \sin\beta \\ -m_Z \sin\theta_w \cos\beta & m_Z \cos\theta_w \cos\beta & 0 & -\mu \\ m_Z \sin\theta_w \sin\beta & -m_Z \cos\theta_w \sin\beta & -\mu & 0 \end{pmatrix} \quad (3{\cdot}11)$$

acting on the vector $(-i\tilde{b}, -i\tilde{w}^3, \tilde{h}_1^0, \tilde{h}_2^0)$. The mass eigenstates of (3·10) and (3·11) are called, respectively, 'charginos' and 'neutralinos' and are denoted $\tilde{\chi}_i^+, \tilde{\chi}_i^0$.

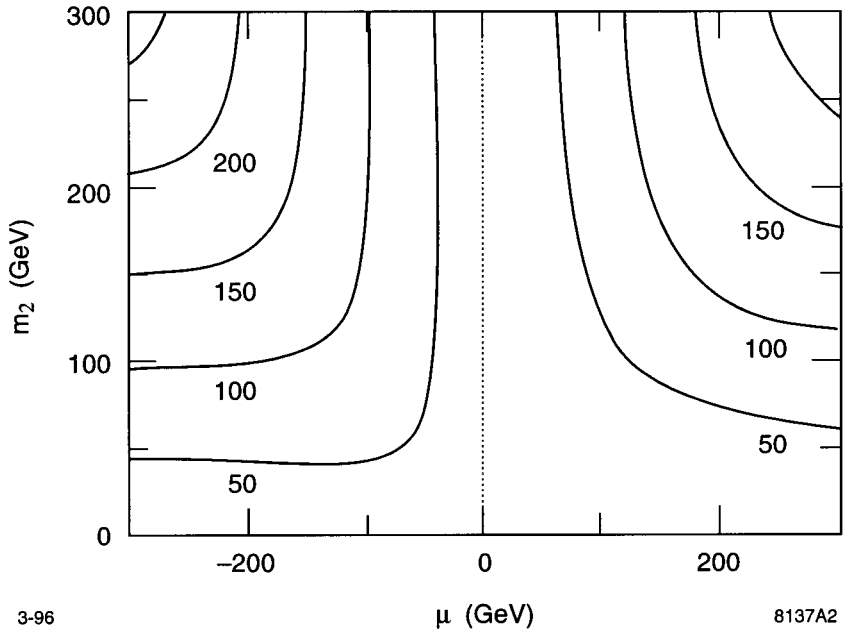


Fig. 2. Lines of constant $\tilde{\chi}_1^+$ mass in the $(m_2, \mu)$ plane, for $\tan\beta = 4$.

One cannot, then, extract $m_1$ and $m_2$ simply by observing the masses of supersymmetric particles. It is also necessary to understand which values of the mixing angles Nature has chosen. Constraints coming from searches for charginos and neutralino are often plotted on the plane of $m_2$ versus $\mu$, at a constant value of $\tan\beta$. The lines in this plane representing constant mass of the lighter chargino, for $\tan\beta = 4$, are shown in Fig. 2. Toward the bottom of this figure, the masses of the lightest charginos and neutralino are close to $m_2$ and $m_1$, and these particles are composed dominantly of the gauge partners. Toward the top of the figure, the lightest chargino and neutralino become degenerate at the value $\mu$ and behave like the partners of Higgs bosons. This means that it is essential, both for the extraction of the supersymmetry breaking parameters and for the more general understanding of the signatures of supersymmetry that experiments should determine where we actually sit in the $(m_2, \mu)$ plane.

### *3.2.* $\tan\beta$

The set of parameters needed for a precise understanding of the spectrum of superpartners also includes $\tan\beta = v_2/v_1$, the ratio of the Higgs field vacuum expectation values. We have already seen that $\tan\beta$ appears as a parameter in the gaugino mixing

problem. This parameter also plays a role in the formula for the scalar masses. Through the supersymmetrization of the gauge interactions, all quark and lepton partners receive a 'D-term' contribution to their masses of the form

$$\Delta m_D^2 = -m_Z^2 \left(\frac{\tan^2\beta - 1}{\tan^2\beta + 1}\right)(I^3 - Q\sin^2\theta_w) \ , \tag{3·12}$$

where $I^3$ and $Q$ are the electroweak quantum numbers.*)

More generally, any discussion of the experimental signatures of supersymmetry brings in many sources of dependence on tan $\beta$, through the production and decay amplitudes for gauginos and Higgs bosons. Thus, it is important to find a model-independent method for determining this parameter.

*3.3. Scalar partner masses*

Once the gaugino mass parameters and tan $\beta$ are determined experimentally, we will have established a proper foundation for a discussion of the spectrum of scalar masses. I will now discuss how the scalar masses can be analyzed, and what variety of patterns the various models of Section 2.2 produce.

In general, the formula for a scalar partner mass has three components. First, there is the underlying supersymmetry-breaking mass term. At least for the light generations, for which we can ignore the Yukawa couplings to the Higgs sector, this term is not renormalized at the level of one-loop renormalization group equations. Second, there is the contribution fed down from the gaugino masses, obtained by integrating the renormalization group equation (3·7). Finally, there is the D-term contribution (3·12). Once tan $\beta$ is known, this last contribution can be computed in a model-independent way and subtracted; I will define the reduced scalar partner masses

$$\overline{m}_f^2 = m_f^2 - \Delta m_D^2(I^3, Q) \ . \tag{3·13}$$

Next, we must deal with the mass contribution due to gauginos. The result of integrating (3·7) can be conveniently written

$$\overline{m}_f^2 = \overline{m}_{f0}^2 + \left(\sum_i 2C_i \frac{\alpha_i^2 - \alpha_{iM}^2}{b_i \alpha_2^2}\right) \cdot m_2^2 \ . \tag{3·14}$$

In this equation, $i$ = 1,2,3 runs over the standard model gauge groups. The $C_i$ are the Casimirs from (3·8). The $b_i$ are the renormalization group coefficients; these are given by $b_i$ = (–33/5, –1, 3) for i = 1,2,3 in minimal supersymmetry. Finally, the $\alpha_{iM}$ are the values of the coupling constants at the messenger scale $M$. In writing this equation, I have assumed gaugino universality to convert the gaugino masses to the single value $m_2$, which should be precisely known. I emphasize again that gaugino universality is an assumption, but one which can be confirmed or refuted experimentally as part of the broader exploration of supersymmetry.

In Section 2.2, the class of models exhibiting dynamical universality included models in which the messengers of supersymmetry breaking were the standard model gauge interactions. In models of this type, gaugino masses are generated directly by one-loop

*) If the theory contains additional gauge bosons, there are additional D terms. I include these in the model-dependent part of the scalar masses.

diagrams involving the supersymmetry breaking sector, and scalar masses are generated at the two-loop level. I have already noted that these models can naturally lead to gaugino unification. A particular model of Dine, Nelson, Nir, and Shirman[20] gives also gives a simple spectrum of scalar masses:

$$\overline{m}^2 = \left(\sum_i 2C_i \frac{\alpha_i^2}{\alpha_2^2}\right) \cdot m_2^2 \; ; \tag{3·15}$$

in this formula, the coefficient 2 depends on the model assumptions, while the general structure is characteristic of this mechanism for the communication of supersymmetry breaking.

The simplicity of the formula (3·15) and its curious resemblance to (3·14) motivates us to consider the following device for exhibiting the spectrum of quark and lepton superpartners. We plot the ratio $\overline{m}/m_2$ against a weighted combination of Casimirs,

$$C = \left(\sum_i C_i \frac{\alpha_i^2}{\alpha_2^2}\right)^{1/2} . \tag{3·16}$$

The prediction of (3·15) is that the superpartner spectrum is a straight line on this plot. Thus it is reasonable to call this device the 'Dine-Nelson plot'.

Models in which the scalar masses come dominantly from the renormalization group effect (3· 14) also have a relatively simple form on the Dine-Nelson plot. In Fig. 3, I have plotted the contributions from renormalization-group running for three values of the messenger scale—a low scale $M$ = 100 TeV, the grand unification scale $2 \times 10^{16}$ GeV, and the fundamental scale of superstring theory, $10^{18}$ GeV. As a comparison, I have also plotted the result (3·15). It is important to note that the Casimir $C$ is not continuously variable but rather takes only fives distinct values, those for the $SU(2)\times U(1)$ multiplets of the standard model, $\ell_R, L_L, d_R, u_R$, and $Q_L$. Of these, the values of $C$ for $d_R$ and $u_R$ (and also the gaugino contributions to their scalar masses) are highly degenerate. So the Dine-Nelson plot is really defined by the value of the masses at these specific points. The curves in Fig. 3 are intended only to guide the eye.

The device of the Dine-Nelson plot gives us a concrete way to view the distinctions between the various classes of models reviewed in Section 2. In Fig. 4, I have plotted the spectrum of quark and lepton partners for each of six representative models. The values of the masses are compared to the position of the top solid curve from Fig. 3, representing the gaugino loop contribution of Fig. 1 integrated from the superstring scale. In supersymmetry phenomenology, the squarks and sleptons of the third generation are often split from the first two due to their coupling to the particles of the Higgs sector. I will ignore that complication here.

Model (a) is a typical model with preset universal scalar masses communicated by supergravity.[17] The values of the masses sit a constant distance in $(\text{mass})^2$ above the solid curve. This increment is positive, so that the theory does not develop an instability at the fundamental scale.*) Notice that the sleptons are typically lighter than the squarks, but the ratio of these masses depends on the size of the original

*) There are realistic models which avoid this constraint in which our vacuum is not the global minimum of the potential but is stable over cosmological time; see Ref. 27.

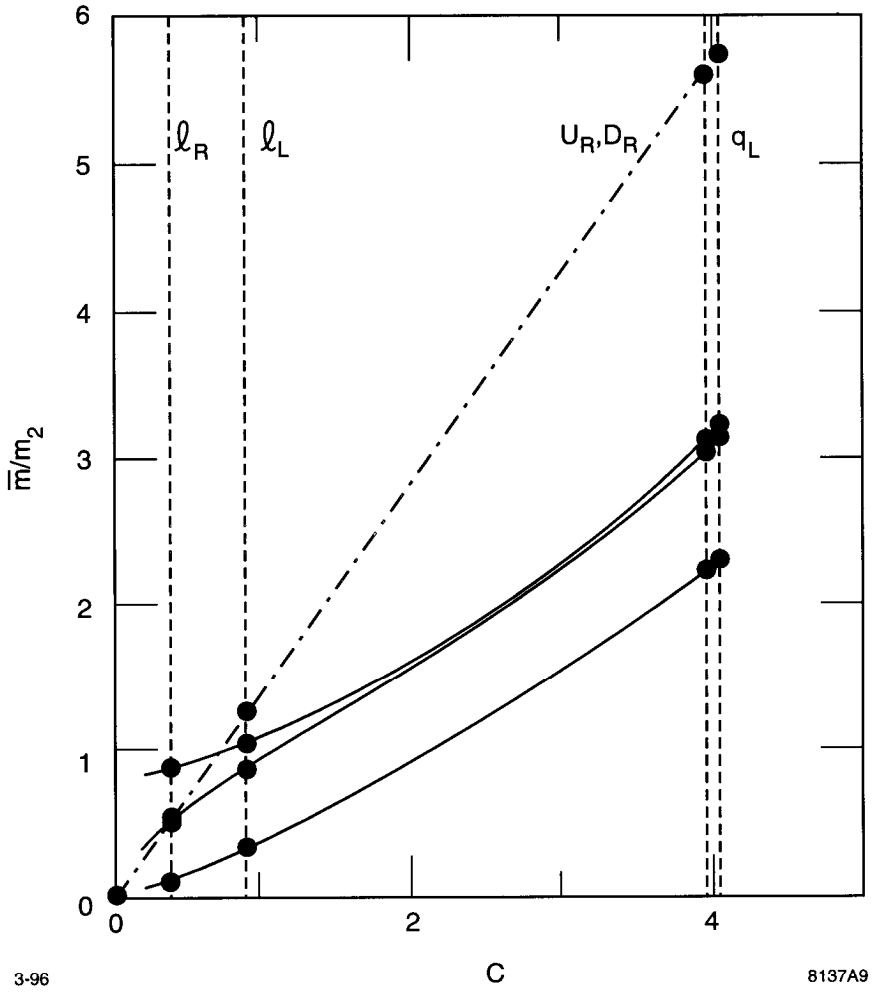


Fig. 3. Some reference models displayed on the Dine-Nelson plot. The solid lines show the integration of the renormalization group equation for two values of the messenger scale. The dotted line shows the linear relation predicted in the model of Dine, Nelson, Nir, and Shirman.

supersymmetry-breaking mass term relative to that generated by renormalization group corrections.

Model (b) is the Dine-Nelson-Nir-Shirman model.[20] I have made some small improvements of the formula (3·15), evaluating the coupling constants at a more realistic scale of about 100 TeV, and then adding the renormalization group enhancements as the masses come down to the weak interaction scale. The dashed line is copied from Fig. 3. Notice that in this class of models the slepton masses are rather small, and also different by a factor 2 between the partners of left- and right-handed leptons.

Model (c) is a variant of the supergravity models which has been considered in Ref. 28. Here the original supersymmetry-breaking scalar masses are universal among generations for a given set of gauge quantum numbers. However, the values of these masses depend on the quantum numbers, for example, differing for the particles that belong to 10 and $\overline{5}$ representations of $SU(5)$. Models in which there are large contri-

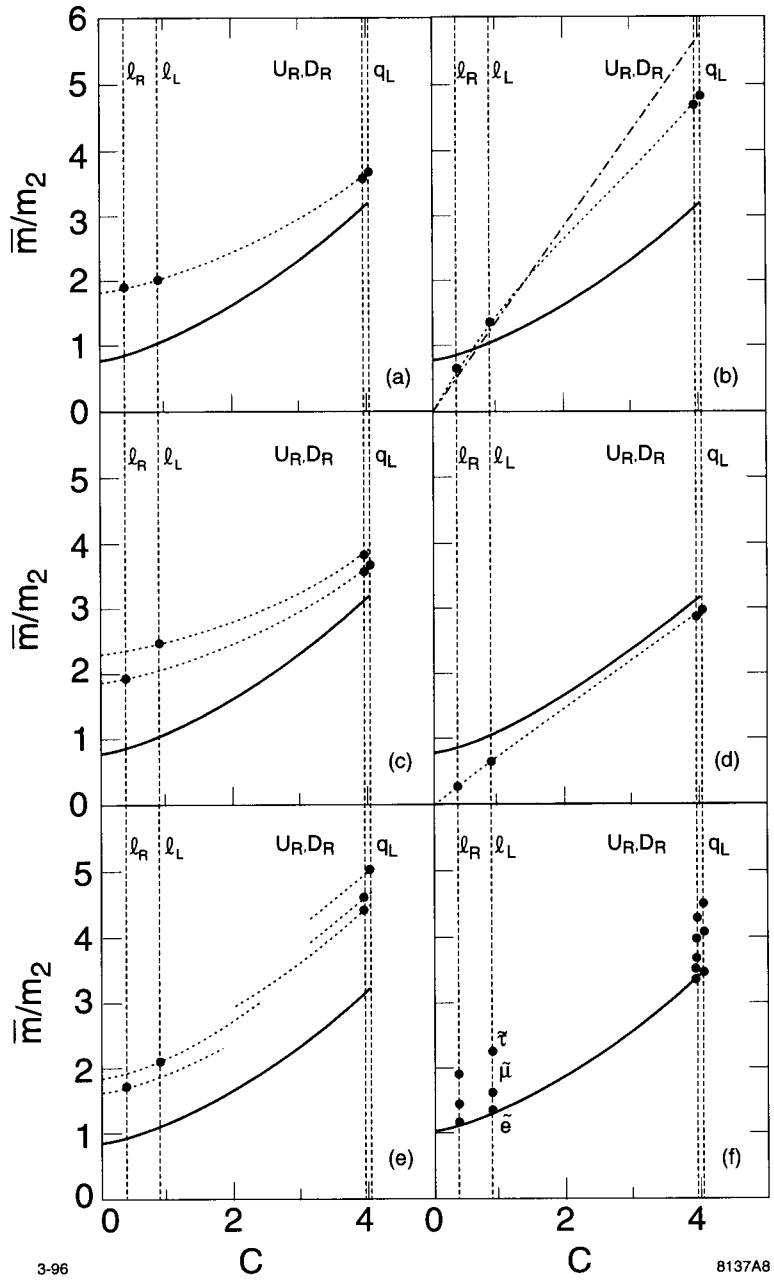


Fig. 4. Six classes of models of supersymmetry breaking, displayed as patterns on the Dine-Nelson plot. The solid reference line is the result of integrating the renormalization group equation from the string scale. The models (a)-(f) are described in the text.

butions to the scalar masses from new D terms due to extended gauge interactions, as in Refs. 29 and 30, and the superstring-based models of Ref. 31, generate patterns similar to these.

Model (d) is a model with dynamical universality presented by Choi.[32] In this model, the original supersymmetry breaking masses are zero, so that the final masses

are determined only by the renormalization group effect, as in 'no-scale' models. However, for Choi, the messenger scale is $F_a$, the axion decay constant, and the messenger interactions are those associated with Peccei-Quinn symmetry breaking.

Model (e) illustrates an idea for dynamical universality due to Lanzagorta and Ross [19] In this model, the supersymmetry-breaking masses are driven to the fixed points of the renormalization group equations for a more complex underlying theory at a high scale. The locations of the fixed points depend on the standard model quantum numbers of the quark and lepton partners, but not on the generation. In principle, the pattern of soft masses is predicted by the underlying model.

Model (f) is an example of a model with preset alignment. In such a scheme, the three supersymmetry-breaking mass parameters for each set of standard-model quantum numbers are distinctly different. Though this is not required in these models, I have drawn the figure to suggest that the masses, for each set of quantum numbers, have an asymptote which is the solid line; this would suggest that the messenger scale is the Planck or string scale, and that the discrete symmetries which regulate the alignment of the mass matrices are characteristic of superstring or other deep-level physics.

Each one of the possibilities presented here is interesting as a plausible model of the origin of supersymmetry breaking. The range of possibilities is fun to think about, and is certainly not exhausted by these cases. That there should be such a wide range is no surprise. In physics, every time we open another door to speculation, manifold possibilities are revealed, and the one chosen by experiment is often one that seemed least likely at the beginning. The real surprise in this figure is how different models of physics coming from a very deep level of Nature present distinctly different patterns. These patterns will be visible in data that can be collected at the weak interaction scale, data that we will gather with the coming generation of high-energy colliders.

### *3.4. Two variant phenomenologies*

Before I discuss how we will collect the information displayed on the Dine-Nelson plot, I should note other some other features of phenomenology which can give insight into the mechanism of supersymmetry breaking. In particular, there are sometimes new reactions which are specific to a particular mechanism of supersymmetry breaking whose observation would give evidence of that mechanism. I will give two examples here.

Barbieri, Hall, and Strumia[33] have noted that, if the lepton superpartners of the three generations receive universal masses at the string scale, the mass matrix of the sleptons grand-unified with the top quark can receive large radiative corrections proportional to the square of the top quark Yukawa coupling. These corrections upset the preset universality and can lead to lepton flavor violation by flavor mixing through the third-generation sleptons. In Ref. 33, the consequences of this idea are worked out for $\mu \to e\gamma$ and other low-energy probes of lepton flavor conservation. In principle, the effect can also be observed directly at colliders. In an $SO(10)$ model which connects the quark and lepton mixing angles, one might estimate

$$\frac{\Gamma(\tilde{\tau}^- \to \mu^- \tilde{\chi}_1^0)}{\Gamma(\tilde{\tau}^- \to \mu^- \tilde{\chi}_1^0)} \sim \left|\frac{m_\tau (A + \mu \tan\beta)}{m_{\tilde{\tau}}^2} V_{cb}\right|^2 \sim 10^{-5} \left(\frac{\tan\beta}{10}\right)^2 \qquad (3\cdot17)$$

for $m_{\tilde{\tau}} \sim A \sim \mu \sim$ 100 GeV. Hall and his collaborators have shown that that the effect can be much larger in other theories of lepton flavor, and that it might also be visible in other reactions. For example, Ref. 34 discusses models in which there are potentially observable signals in $e^+e^- \to e^+\mu^-\tilde{\chi}_1^0\tilde{\chi}_1^0$ and in $e^-e^- \to e^-\mu^-\tilde{\chi}_1^0\tilde{\chi}_1^0$.

Another interesting possibility arises in model in which supersymmetry is broken by gauge theory dynamics at energies relatively close to the weak scale. In any model with spontaneously broken supersymmetry, each pair of superpartners couples to the Goldstone fermion of supersymmetry. For example, assuming that the $\tilde{b}$ is an approximate mass eigenstate, this particles couples to the photon and the goldstino $(\tilde{g})$ by

$$\Delta \mathrm{L} = \frac{\cos\theta_w m_{\tilde{b}}}{\Lambda^2}\bar{\tilde{b}}\sigma^{\mu\nu}F_{\mu\nu}\tilde{g} \ , \tag{3·18}$$

where $\Lambda$ is the mass scale of symmetry breaking. In supergravity, the goldstino is eaten by the gravitino, which obtains a mass of order $\Lambda^2/m_{\mathrm{Pl}}$. For values of $\Lambda$ near the unification scale, the coupling (3. 18) is completely irrelevant to particle physics experiments. However, as $\Lambda$ comes below 100 TeV, the decay $b \to \gamma\tilde{g}$ can occur inside a collider detector, leading to observable reactions with direct photons such as $e^+e^- \to \gamma\gamma\tilde{g}\tilde{g}$[35] and $e^+e^-, q\bar{q} \to \tilde{e}^+\tilde{e}^- \to e^+e^-\gamma\gamma\tilde{g}\tilde{g}$.[36]

The observation of either of these interesting supersymmetry phenomena would single out particular models from among the many classes that we are considering here. In the remainder of this paper, however, we will consider only the most conservative picture of supersymmetry reactions and concentrate on the question of how we can assemble the spectral data needed to construct the Dine-Nelson plot.

## §4. Experiments at Hadron Colliders

In the previous section, I have set out a systematic but somewhat idealized experimental program aimed at establishing the mechanism of supersymmetry breaking. In this program, one must first set the scale of supersymmetry partner masses by measuring the gaugino masses and testing gaugino universality. Then one must identify the scalar states associated with each flavor and helicity of quarks and leptons, and we must measure their masses with sufficient precision to recognize their pattern on the Dine-Nelson plot. In this section and the next, I will compare this idealized program with the realistic expectations for experiments at future colliders.

Though it is important to recognize that supersymmetry might be discovered in next few years at LEP II or at the Tevatron, so that the experimental study of supersymmetry could begin with the current generation of accelerators, I will concentrate my discussion on the expectations for the accelerators of the next generation. On the side of hadron colliders, I will discuss studies done for the LHC; on the side of lepton colliders, I will discuss the expectations for $e^+e^-$ linear colliders. Some results on supersymmetry parameter determination specifically directed to the LEP II program have been discussed in Refs. 37 and 38.

In this section, then, I will present the aspects of our general program which are discussed in simulation studies of supersymmetry experiments for the LHC. These studies have, for the most part, been directed to shorter-term goals than the ones I have emphasized here, to the first discovery of supersymmetry, rather than to the

systematic experiment al pursuit of the new physics. In fact, it should be easy for the LHC to discover supersymmetry. The cross section for gluino pair production in hadronic collisions is an order of magnitude larger than that for production of a quark of comparable mass, and the expected signature of multijet events with large missing energy is striking and characteristic.

Togo deeper than the observation of anomalies, however, will be difficult at hadron colliders. The reasons for this do not come from considerations of relative cleanliness and such experimental matters which are debated between the hadron and lepton physics communities. Rather, they come from the specific predictions of supersymmetry phenomenology. The difficulties and the promise of hadron collider experiments can be made clearer by reviewing some of the techniques which have been developed to date for obtaining information on the supersymmetry spectrum in this environment.

Before beginning this review, I would like to recall the expectation, both in this generation of accelerators and the next, that hadron and lepton collider experiments should probe roughly the same regions of the parameter space of supersymmetry. The reason for this is that colored superpartners receive large positive mass enhancements from their coupling to gluons and gluinos. This is most clear in the gaugino sector. I argued in Section 3.1 that gaugino unification should at least be a useful guide to the general properties of the supersymmetry spectrum. According to (3·9), the short-distance gluino mass $m_3$ should be roughly three times the mass parameter $m_2$. To convert to physical mass values, we must note that $m_2$ is essentially an upper bound to the lightest chargino mass, while $m_3$ receives a 15% upward radiative correction when converted to the 'pole' mass which determines the kinematics of gluino production. Another similarly large correction, which may be of either sign, may appear if the gluino and squark masses differ by a large ratio.[24] Thus,

$$m(\tilde{g}) > 3.5(m(\tilde{\chi}_1^+)^2 - m_W^2)^{1/2} \ . \tag{4·19}$$

Thus, a chargino discovery at 80 GeV which might be made at LEP 2 would correspond to a gluino at 300 GeV which might be discovered at the Tevatron. A linear collider at 1 TeV would be able to search for charginos up to 500 GeV; the corresponding gluino mass is 1700 GeV, which is roughly the search limit of the LHC if $m_{\tilde{g}} \ll m_{\tilde{q}}$.[40] Both of these values are a factor of two beyond the naturalness limits given in (2·1). In a similar way, the sleptons are expected to be lighter than the squarks, though the precise relation is more model-dependent. Fig. 4 contains spectra in which the ratio of squark to right-handed slepton masses varies from 2 to 6. Of course, this correspondence does not mean that the hadron and lepton colliders are competing to discover the same information. In fact, as we will see, quite the reverse is true.

Hadron colliders provide many striking signatures of supersymmetry. The most basic signature is that of missing energy in multijet events. But the production of supersymmetric particles can also lead to interesting multilepton and $Z^0$ plus lepton topologies. A summary of event rates at the LHC for a variety of increasingly exotic reactions is shown in Fig. 5.[41] These exotic final states arise from decays in which the gluino or squark which is the primary product of the hadronic reaction decays to a neutralino or chargino, which then decays by a cascade to reach the lightest

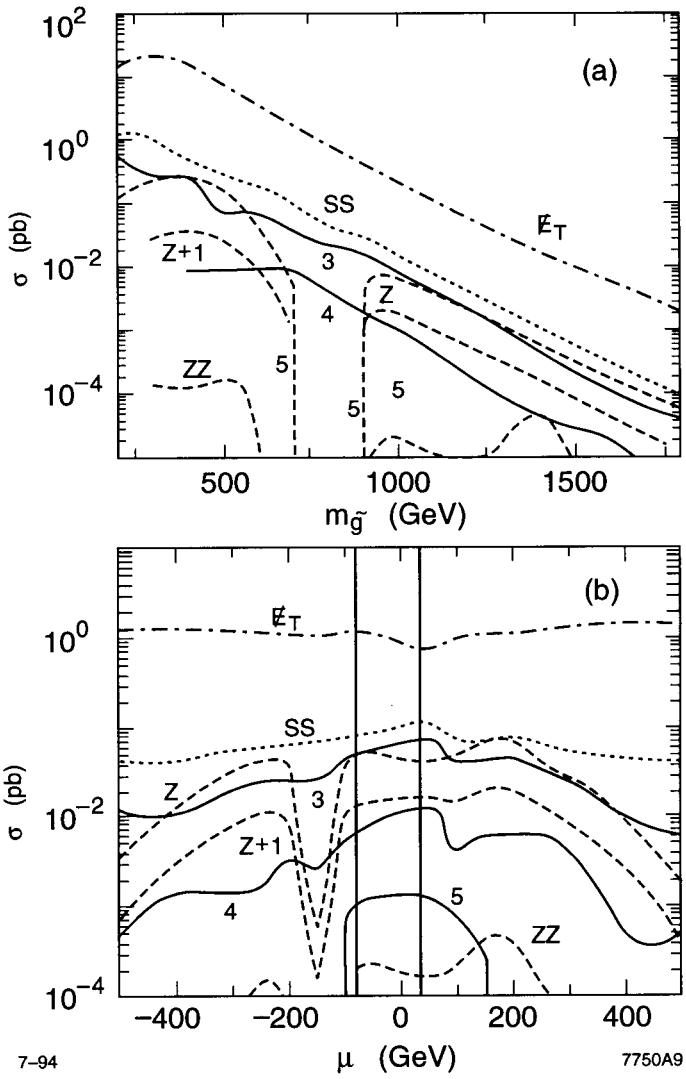


Fig. 5. Cross sections for various signatures of supersymmetry observable at the LHC, from Ref. 41. The various curves give the cross sections for missing transverse energy, same-sign dilepton production, multilepton events, and multilepton + $Z$ events. The cross sections are shown (a) as a function of the mass of the gluino, for $m(\tilde{g}) = m(\tilde{q})/2$ and $\mu = -150$ GeV, (b) as a function of the parameter $\mu$ for a fixed gluino mass equal to 750 GeV.

superparticle.[42] An example of such a cascade decay is

$$\begin{aligned} pp \to \quad & \tilde{g} \to q\bar{q} + \tilde{\chi}_2^+ \to \ell^+\nu + \tilde{\chi}_2^0 \to q\bar{q} + \tilde{\chi}_1^0 \\ & + \tilde{g} \to q\bar{q} + \tilde{\chi}_3^0 \to Z^0 + \tilde{\chi}_1^0 \end{aligned} \tag{4·20}$$

The appearance of these many topologies is a strength of the hadronic window into supersymmetry, but it is also its weakness. First, because superpartners are pair-produced, and each partner decays with missing energy, it is not possible to reconstruct a superpartner as a mass peak. The reaction shown in (4·20) illustrates that supersymmetry reactions can contain sources of missing energy from $\nu$ or $Z^0$ emission in

addition to that from the final neutralino. Of course, in hadronic collisions, the initial parton energies and polarizations are also unknown. Thus, analyses of supersymmetry parameters must be based on overall hadronic reaction rates, or on other observable which integrate over the underlying kinematic parameters. To interpret such variables, one needs a trustworthy model of the reaction being studied. But now we come to the second problem. The pattern of squark and gluino decays is influenced by the spectrum and mixings of charginos and neutralino and changes as the parameters of these states move in the $(m_2, \mu, \tan\beta)$ space. If one relies only on data from hadronic supersymmetry processes, the dependence on these parameters enters as an essential modelling ambiguity.

To clarify these issues, I would like to describe a number of methods proposed in the literature for the detailed measurement of supersymmetry parameters. Before turning to strongly interacting particles, I will comment on color neutral states. Hadronic collisions can also access the chargino and neutralino states directly, through the reactions

$$q\bar{q} \to \tilde{\chi}^0\tilde{\chi}^0, \qquad q\bar{q} \to \tilde{\chi}^0\tilde{\chi}^+ \ . \tag{4·21}$$

The second of these reactions is a potential source of trilepton events, and therefore has been discussed as an interesting mode for the discovery of supersymmetry at the Tevatron collider.[44] Baer and collaborators have noticed that this reaction can also give some spectral information: The dilepton spectrum in trilepton events falls off sharply at dilepton masses equal to the mass difference $m(\tilde{\chi}_2^0) - m(\tilde{\chi}_1^0)$, allowing a measurement of this parameter of the neutralino mass matrix.[45] Sleptons can also be discovered at hadron colliders. An analysis of the slepton signal at LHC, using as the signature acoplanar isolated leptons, is given in Ref. 43. This signal unfortunately has a very low rate, and also sums the contributions of the partners of left- and right-handed sleptons, so it is not promising for an accurate mass determination.

For the strongly interacting superpartners, we should hope that the hadron colliders can give us accurate mass measurements. Let us consider first the gluino mass measurement. This is simplest if the supersymmetry parameters are such that $m_{\tilde{g}} < m_{\tilde{q}}$, and I will restrict my attention to that case for a moment. There is one proposed estimator for the gluino mass that does peak sharply, proposed some time ago by Barnett, Gunion and Haber.[46] These authors suggested that one should select events with like-sign dileptons and combine a lepton momentum with the momentum vectors of the nearest appropriately hard jets. The resulting mass distribution roughly tracks the gluino mass and has a width of about 15%. Baer, Chen, Tata, and Paige have criticized this analysis for omitting some backgrounds, but have introduced their own observable applicable simply to missing energy events.[47] In events with missing transverse energy greater than some criterion $E_T^c$, and with two jets in one hemisphere with transverse energy greater than $E_T^c$, they examine the mass distribution of these two jets. Mass distributions generated by Monte Carlo are shown in Fig. 6 for sets of three values of the gluino mass differing by 15%. This analysis makes plausible that such integral variables can produce a gluino mass estimate of reasonable accuracy.

In order to understand whether the gluino is in fact lighter than the squarks, and to measure the mass ratio, a number of techniques can be employed. For example, the $\tilde{q}_R$ typically decays dominantly into the lightest neutralino, so if these particles are light the missing energy signature is stronger and the jet multiplicity is smaller. The use of

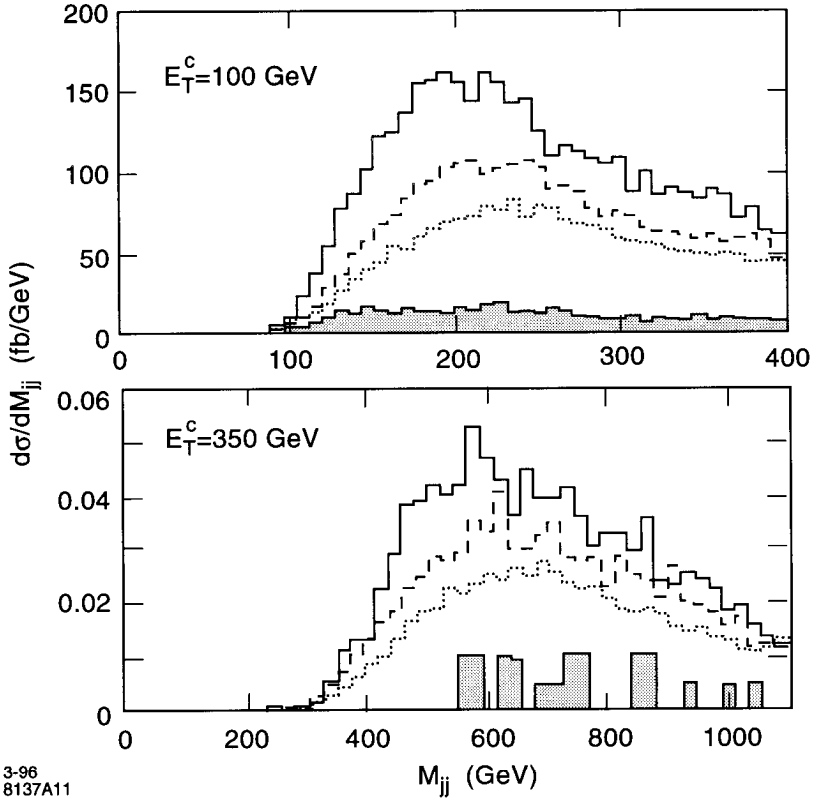


Fig.6 Mass distribution of the estimator of Baer *et al.*, Ref. 47, for two different ranges of gluino mass: (a) using $E_T^c$ = 100 GeV, the distributions are shown for $m(\tilde{g})$ = 296, 340, 369 GeV; (b) using $E_T^c$ = 350 GeV, the distributions are shown for $m(\tilde{g})$ = 773, 885, 966 GeV. The simulation assumes that the squarks are much heavier than the gluinos.

jet multiplicity to probe the ratio of the squark and gluino masses in discussed in Ref. 47. An additional amusing probe of the squark-gluino mass ratio has been studied by Basa[48] and by the ATLAS collaboration.[40] If squarks and sleptons are comparable in mass, one of the major processes for supersymmetry production at the LHC is

$$q + q \to \tilde{q}\tilde{q} \tag{4·22}$$

by *t*- channel gluino exchange. Since there are more up quarks than down quarks in the proton, this reaction produces an excess of $\ell^+\ell^+$ over $\ell^-\ell^-$ like-sign dilepton events. The asymmetry peaks when the squark and gluino masses are roughly comparable, as shown in Fig. 7. On the other hand, the total rate of like-sign dilepton events falls as the gluinos become heavier than the squarks. Thus, it is possible at least in principle to determine the mass ratio from these two pieces of information.

These observable give the flavor of supersymmetry mass determinations in hadronic collisions. There will be considerable information available, if one can learn how to use it. This information resides in integrated reaction rates for various supersymmetry production processes, and in the rates of exotic multilepton reactions. Unfortunately, the spectral pattern is coupled in these observable to the detailed model of squark and

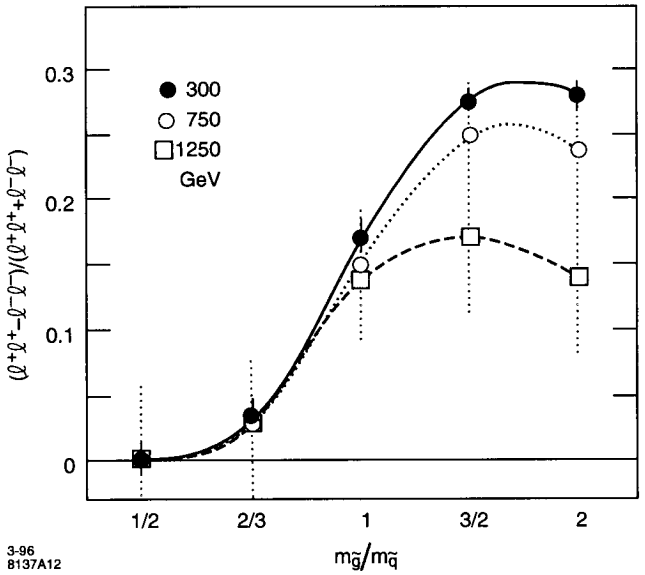


Fig. 7. Dependence of the asymmetry between dilepton events with $\ell^+\ell^+$ to those with $\ell^-\ell^-$, as a function of the mass ratio of the squark and gluino, from Ref. 40. The three curves represent three different values of the lighter of the gluino and quark masses.

gluino decay, which contains the full complexity of the chargino and neutralino mixing problem.

The task of separating these components and extracting the supersymmetry mass parameters purely from hadronic cross sections seems like a nightmare. In fact, none of the analyses I have just described have yet been carried out as systematic surveys over parameter space. It is not so easy to choose a parameter space of sufficiently low dimension that it can be surveyed systematically.

Fortunately, the situation looks much brighter if it is assumed that there will be an $e^+e^-$ linear collider operating in the same time period as the LHC. I will explain in the next section that experiments at $e^+e^-$ colliders in provide an array of tools to accurately measure not only the chargino and neutralino masses but also their mixing angles. Thus, these experiments will provide the values of the underlying supersymmetry parameters needed to explicitly model squark and gluino decays. Armed with this model, experimenters at the LHC will be able to convert their integrated observable into constraints on the spectrum of squark and gluino masses. In this way, the extensive energy reach of the LHC can be used effectively to provide values of the squark and gluino masses, in a range well beyond the reach of the $e^+e^-$ colliders, to accuracies of 10-15%.

## §5. Experiments at $e^+e^-$ Colliders

Now I will turn to a review of the expectations for supersymmetry experiments at the proposed $e^+e^-$ linear colliders which should carry electron-positron experimentation to the next step in energy. For concreteness, I will have in mind a linear collider with a center-of-mass energy of 500 GeV and a design luminosity of 50 $\text{fb}^{-1}$/ yr; this accords

with the current SLAC and KEK designs. These designs evolve smoothly to 1 TeV in the center of mass; the corresponding reach of almost 500 GeV in the chargino mass covers a region of parameter space comparable to that covered by the LHC, as I have noted above. A more general review of the capabilities of $e^+e^-$ linear colliders can be found in Ref. 6.

*5.1. Gaugino masses*

I will begin by discussing $e^+e^-$ experiments on charginos and neutralino. In the estimate (2·1), I noted that the lighter chargino and neutralinos are likely be among the lightest particles of the supersymmetry spectrum. We can then use the reactions of these particles to determine the gauginos masses $m_1$ and $m_2$, and also to learn more detailed information about the values of the general parameters of the supersymmetric model.

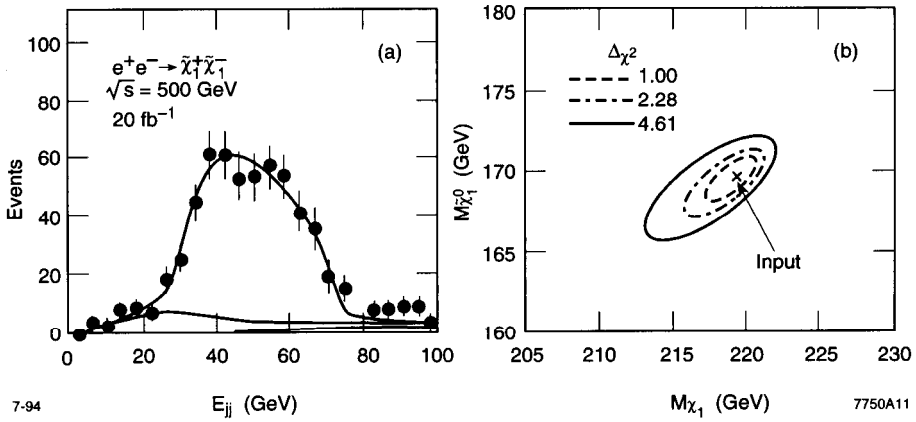


Fig. 8. Determination of the lightest chargino mass in the decay $\tilde{\chi}_1^+ \to q\bar{q}\tilde{\chi}_1^0$, according to the simulation results of Ref. 25. The right-hand figure shows the $\chi^2$ distribution as a function of the masses of $\tilde{\chi}_1^+$ and $\tilde{\chi}_1^0$.

If the lighter chargino is lighter than the sleptons, it will decay via

$$\tilde{\chi}_1^+ \to \ell^+\nu\tilde{\chi}_1^0 , \qquad \tilde{\chi}_1^+ \to q\bar{q}\tilde{\chi}_1^0 .$$

Imagine, then, selecting events with the reaction $e^+e^- \to \tilde{\chi}_1^+\tilde{\chi}_1^-$ in which one chargino decays to quarks and the other to leptons. The invariant mass of the $q\bar{q}$ system has a predictable distribution whose kinematic endpoints determine the mass of the parent $\tilde{\chi}_1^+$ and the mass of the $\tilde{\chi}_1^0$ into which it decays. Simulations of the reconstruction of this distribution at future linear colliders show that these masses can be determined quit e accurately. For example, in the simulation shown in Fig. 8, these two masses are determined to 3% accuracy.

I have stressed in Section 3.1, however, that the determination of the masses of charginos and neutralino is only the beginning of what is needed. In order to determine the underlying supersymmetry breaking parameters of the theory, and to resolve the problem of cascade decays which enters the analysis of the signatures of supersymmetry in *pp* collisions, we must also determine the mixing angles which arise when the mass matrices are diagonalized. Fortunately, lepton colliders offer particular incisive tools

which allow one to analyze the mixing of chargino and neutralino states. I will now present two techniques for doing this. In this discussion, I will discuss the formulae for $e^+e^-$ cross sections to supersymmetric particle pairs, but only in a rather schematic way. A very useful compilation of the formulae for supersymmetry production in $e^+e^-$ reactions can be found in Ref. 49.

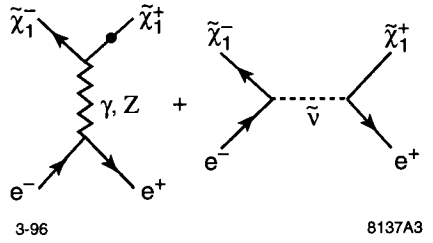


Fig. 9. Diagrams contributing to the process $e^-e^+ \to \tilde{\chi}_1^+\tilde{\chi}_1^-$.

We first consider the reaction $e^-e^+ \to \tilde{\chi}_1^+\tilde{\chi}_1^-$, making use of the highly polarized electron beams which are anticipated for linear collider experiments. In Ref. 25, some wonderful observations are made about this process. To understand these, imagine first that we study the reaction at very high energy, so high that we can ignore all masses. Now assume that the electron beam can be polarized completely in the right-handed orientation. Since right-handed electrons do not couple to the $SU(2)$ gauge interactions, the second diagram in Fig. 9 vanishes. In addition, the first diagram in Fig. 9 involves only the linear combination of $\gamma$ and $Z^0$ which gives the $U(1)$ (hypercharges) gauge boson. But the $U(1)$ gauge boson does not couple to $W$ superpartners. Thus, this diagram only involves the Higgs superpartners. If we project onto the lowest mass eigenstate, the rate of the process $e_R^-e^+ \to \tilde{\chi}_1^+\tilde{\chi}_1^-$, will be proportional to the squares of the mixing angles linking the $\tilde{h}_1^-$ and $\tilde{h}_2^-$ to this mass eigenstate.

The promise which is suggested by this high-energy analysis is actually realized under more realistic conditions. In Fig. 10, I plot contours of this polarized cross section for an $e^+e^-$ collider at 500 GeV in the relevant region of the $(m_2, \mu)$ plane. You can see that the cross section maps out this plane, giving the location chosen by Nature, up to a two-fold $(\mu \leftrightarrow -\mu)$ ambiguity, for any determined value of the chargino mass.

Actually the chargino pair production cross section contains even more information. Going back to the limit of very high energies, the angular distribution for an $e_R^-$ to produce a right-handed fermion is proportional to $(1 + \cos\theta)^2$, while the angular distribution to produce a left-handed fermion is $(1 - \cos\theta)^2$. Thus, the forward production of $\tilde{\chi}_1^-$ is given by the mixing angle for $\tilde{h}_2^+$, while the backward production is controlled by the mixing angle for $\tilde{h}_1^-$. Thus, measurement of both the total cross section and the forward-backward asymmetry for this process gives the two mixing angles needed to diagonalized the chargino mass matrix (3.10). In this analysis, one must assume that there are only two of Higgs doublets that the weak scale (as is required for the grand unification of couplings), but there are essentially no other model-dependent assumptions. The expected constraints on the two mixing angles, for a particular point studied in the simulations of Ref. 50, are shown in Fig. 11.

A second method for determining the gaugino mixing parameters involves the pro-

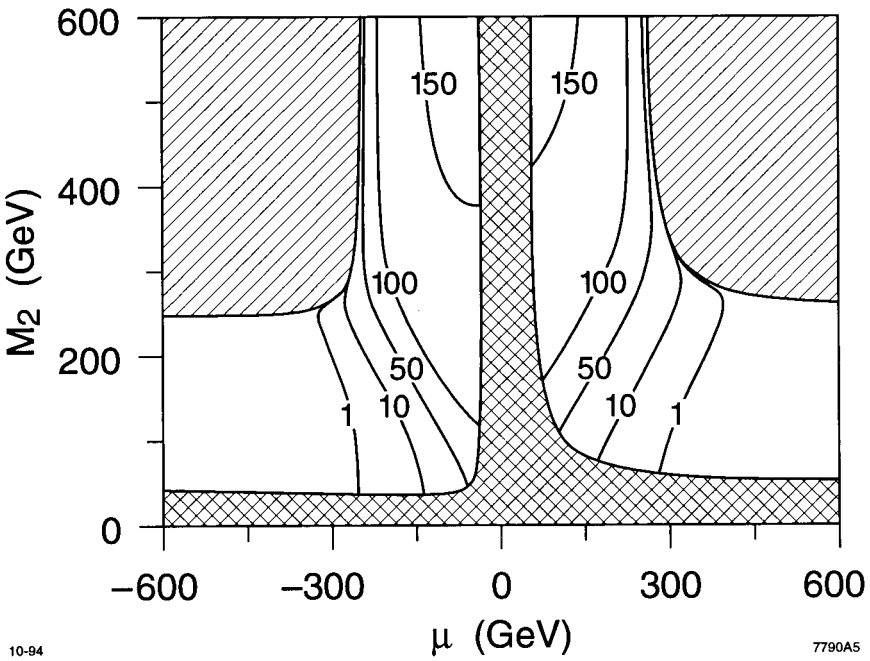


Fig. 10. Total cross section for the process $e_R^- e^+ \to \tilde{\chi}_1^+ \tilde{\chi}_1^-$, in fb, as a function of $m_2$ and $\mu$, for $\tan\beta = 4$, from Ref. 25. The selected region is that in which the lightest chargino is too heavy to have been discovered at the $Z^0$ but is accessible to a 500 GeV $e^+e^-$ collider.

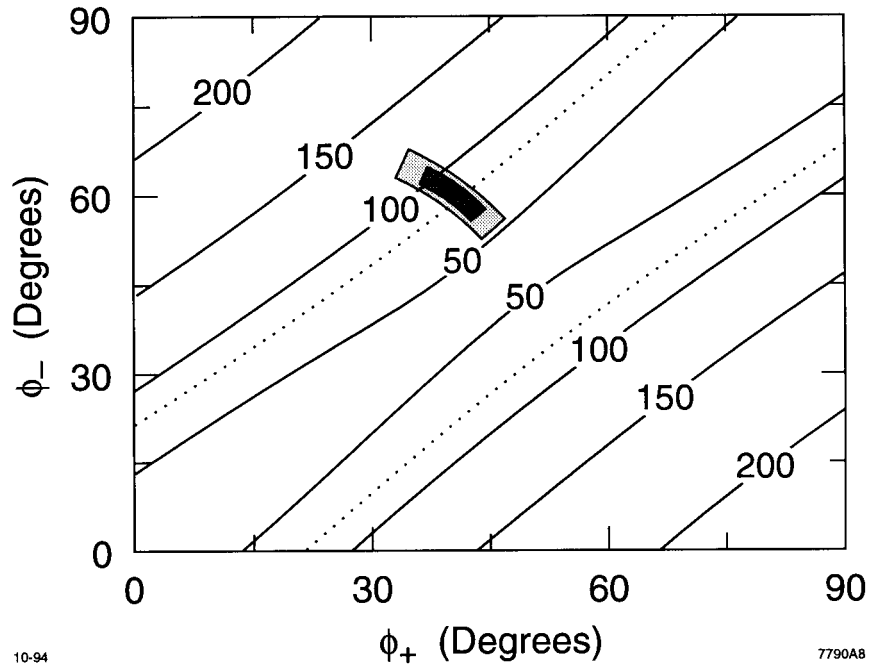


Fig. 11. Determination of the two mixing angles of the chargino mass matrix from the two chargino masses and the total cross section and forward-backward asymmetry for $e_R^+ e^- \to \tilde{\chi}_1^+ \tilde{\chi}_1^-$, according to the simulation results of Ref. 50. The larger box represents the constraint from 30 $\text{fb}^{-1}$ of data, the smaller box from 100 $\text{fb}^{-1}$.

duction of electron partners, selections. There are two selections, one the partner of $e_R^-$, the other the partner of $e_L^-$. (These states can be easily distinguished by the polarization asymmetry of their production in $e^+e^-$ reactions.) I will discuss the event selection and mass measurement for selections in Section 5.3. For the moment, we need only note that the selections are expected, in all of the models shown in Fig. 4, to have masses comparable to that of the lightest chargino, so that they should also be found in the early stages of the experimental program at a linear collider.

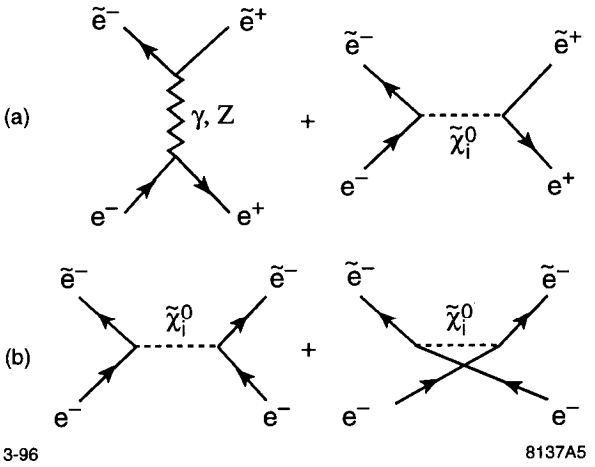


Fig. 12. Diagrams contributing to the processes (a) $e^-e^+ \to \tilde{e}^-\tilde{e}^+$; (b) $e^-e^- \to \tilde{e}^-\tilde{e}^-$.

The Feynman diagrams which contribute to selectron production in $e^+e^-$ annihilation are shown in Fig. 12(a). The second diagram involves neutralino exchange. Although this diagram is exotic, it typically dominates, since the lightest neutralino is usually lighter than the $Z^0$ and the diagram is a t-channel rather than an s-channel exchange. A related process is that of selectron production in $e^-e^-$ collisions. Here the reaction is mediated only by neutralino exchange diagrams, in the *t*- and *u*- channel.

To discuss these processes, it is convenient to define 'neutralino functions', in the following way: Let $V_{ij}$ be the orthogonal matrix that diagonalized (3.11), with the first index denoting a weak eigenstate and the second denoting a mass eigenstate. Define

$$V_{Ri} = -\frac{1}{\cos\theta_w} V_{1i}$$
$$V_{Li} = -\frac{1}{2\cos\theta_w} V_{1i} - \frac{1}{2\sin\theta_w} V_{2i} \ . \qquad (5{\cdot}24)$$

Then define, for $a, b = L, R$,

$$\mathbf{N}_{ab}(t) = \sum_i V_{ai} \frac{m_1^2}{m_i^2 - t} V_{bi}$$
$$\mathbf{M}_{ab}(t) = \sum_i V_{ai} \frac{m_1 m_i}{m_i^2 - t} V_{bi} \qquad (5{\cdot}25)$$

where the sum runs over the four neutralino mass eigenstates, $m_i$ is the mass of the $i$th neutralino, and $m_1$ has been introduced to make the functions dimensionless. The

neutralino functions are simply related to the production cross sections, for example,

$$\frac{d\sigma}{d\cos\theta}(e_R^- e^+ \rightarrow \tilde{e}_R^- \tilde{e}_R^+) = \frac{\pi\alpha^2}{4s}\left[1 + \frac{\sin^2\theta_w}{\cos^2\theta_w}\frac{s}{s-m_Z^2} - \frac{s}{m_1^2}\mathbf{N}_{RR}(t)\right]^2 \beta^3 \sin^2\theta \ . \qquad (5{\cdot}26)$$

The functions $\mathbf{N}_{RR}, \mathbf{M}_{RL}, \mathbf{N}_{LL}$ enter the formulae for the production of $\tilde{e}_R^- \tilde{e}_R^+, \tilde{e}_R^- \tilde{e}_L^+$, and $\tilde{e}_L^- \tilde{e}_L^+$, respectively, in $e^+e^-$ annhiliation; the opposite three combinations enter into the production cross sections for $e^-e^-$.

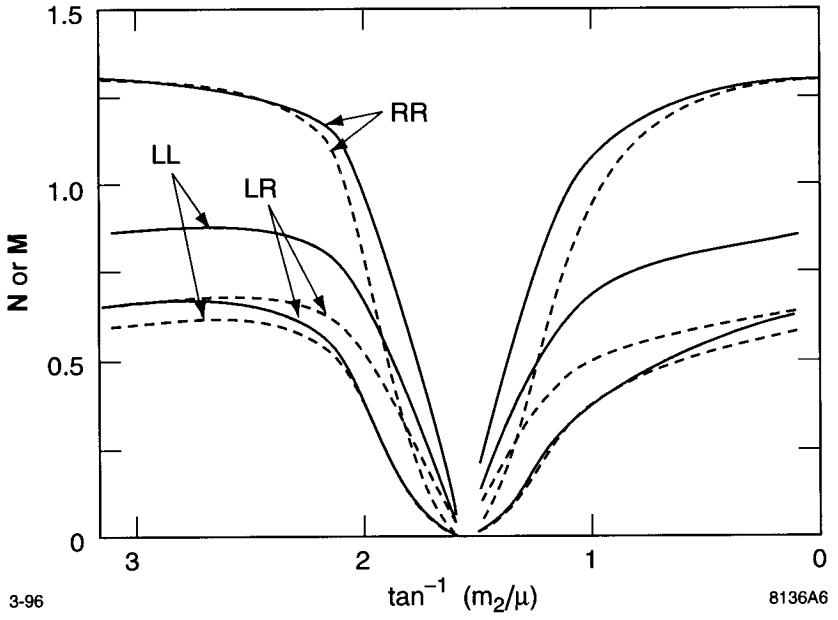


Fig. 13. Values of the 'neutralino functions' $\mathbf{N}_{ij}, \mathbf{M}_{ij}$, at $t = 0$, as a function of the angle in the $(m_2, \mu)$ plane: $\alpha = \tan^{-1}(\mu/m_2)$. The solid curves denote the predictions for selectron production in $e^+e^-$ collisions, the dotted curves for selectron production in $e^-e^-$ collisions.

The neutralino functions are full of information about the neutralino mixing problem. As an example, I plot in Fig. 13 the values of the six neutralino functions, extrapolated to $t = 0$, along a contour of constant chargino mass in the $(m_2, \mu)$ plane. These variables also map the position in this plane. Though it is not shown here, the relative heights of the curves are sensitive to the value of $m_1/m_2$ and thus provide a test of gaugino unification. A detailed simulation of selectron pair production which uses these ideas to extract $m_1, m_2$ and $\mu$ has been presented in Ref. 25. The results of that paper, which assume 50 $\text{fb}^{-1}$ of data, correspond to a test of the gaugino unification of $m_1$ and $m_2$ at the 5% level.

### 5.2. $\tan\beta$

Unfortunately, there is no method known which systematically determines $\tan\beta$ throughout its whole range of possible values. I will discuss here four methods, of which the first two apply mainly for small or intermediate values of $\tan\beta$ and the last two

require probes at higher energy. It is likely that some combination of these methods can determine $\tan\beta$ well enough to interpret experimental data on the superparticle spectrum.

The first method for determining $\tan\beta$ goes back to the chargino production cross section discussed in Section 5.1. I argued there that it is possible to determine the mixing angles needed to diagonalized the chargino mass matrix; from these, one can deduce the off-diagonal elements of this mass matrix. But note from (3·10) that the ratio of these elements is just equal to $\tan\beta$. Since these off-diagonal elements are related by supersymmetry to the vertices which give mass to the $W$ boson, this ratio is model-independent. In Ref. 50, it was remarked that the determination of the chargino mass matrix discussed there could be interpreted as a $\tan\beta$ measurement. Then this parameter could be determined with an accuracy of was 3% at $\tan\beta = 4$, for a parameter set in which the lightest chargino was a roughly equal mixture of gaugino and Higgsino.

A second method for determining $\tan\beta$ has been proposed by Nojiri.[51] This involves a beautiful supersymmetry observable for linear colliders, the polarization of the $\tau$ leptons produced in $\tilde{\tau}$ decay. The $\tau$ polarization is now known to be straightforwardly measurable in $e^+e^-$ experiments. The polarization of $\tau$'s from $\tilde{\tau}$ decay contains information on the mixing of the two $\tilde{\tau}$ eigenstates and on the decay pattern. For a full discussion of the extraction of this information, see Ref. 51. For the purpose of this discussion, I will simply point out that the mixing of $\tilde{\tau}_L$ and $\tilde{\tau}_R$ can be determined from the $\tilde{\tau}$ cross sections and polarization asymmetry. In the following discussion, I will assume for simplicity that the lightest $\tau$ partner is an unmixed $\tilde{\tau}_R$.

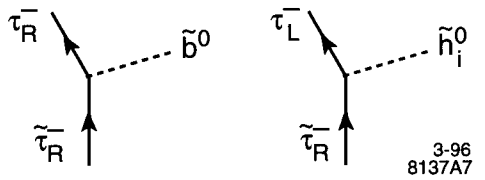


Fig. 14. Components of the decay $\tilde{\tau}_R \to \tau\tilde{\chi}_1^0$.

The dominant decay of this scalar should be to $\tau\tilde{\chi}_1^0$. In terms of weak-interaction eigenstates, there are two amplitudes that contribute to this decay; these are shown in Fig. 14. On one hand, the $\tilde{\tau}_R^-$ can decay to a $\tau_R^-$ with the emission of a $\tilde{b}^0$. On the other hand, the $\tilde{\tau}_R^-$ can decay to a $\tau_L^-$ with the emission of a $h_1^0$. These two processes give rise to a nontrivial $\tau$ polarization, given to first order by

$$P(\tau^-) = 1 - \frac{\cos^2\theta_w}{\sin^2\theta_w}\frac{m_\tau^2}{m_W^2}\frac{1}{\cos^2\beta}\frac{p(\tilde{h}_1^0)}{p(\tilde{b}^0)}\ , \qquad (5\cdot27)$$

where $p(\tilde{h}_1^0)$ and $p(\tilde{b}^0)$ are the probabilities that the lightest neutralino appears as one of these states. If we know the content of the lightest neutralino mass eigenstate in terms of weak eigenstates—and I have given methods for determining this in the previous section—this formula can be solved for $\cos\beta$. This technique should give $\tan\beta$ measurements below the 10% level even when the Higgsino component of the lightest neutralino is rather small.

Ideally, tan $\beta$ can be determined from the branching ratios of the heavy Higgs bosons of supersymmetry. If the $A^0$ boson of the Higgs sector has a mass well above the $Z^0$ mass, the lightest Higgs boson $h^0$ has branching ratios close to those of the Higgs boson of the minimal standard model. However, the heavy Higgs bosons $H^0$ and $A^0$ have couplings which reflect the ratio of the two Higgs vacuum expectation values. For example,

$$\frac{\Gamma(H^0 \to t\bar{t})}{\Gamma(H^0 \to b\bar{b})} = \left(\frac{m_t}{m_b}\cot^2\beta\right)^2\left(1 - \frac{4m_t^2}{m_H^2}\right)^{1/2} . \tag{5·28}$$

Unfortunately, these heavy Higgs bosons have masses of order 500 GeV in typical models, and they must be pair-produced (except in $\gamma\gamma$ collisions); thus, they may be difficult to find in the early stages of linear collider experimentation.

As a last resort, there is one interesting determination of tan $\beta$ that will be available from the LHC. The processes $H^0, A^0 \to \tau^+\tau^-$ is a possible mode for observing the heavy Higgs bosons at the LHC, but only if the branching ratios to $\tau^+\tau^-$ are enhanced by a large value of tan $\beta$.[39,40] If this signature can be observed, then tan $\beta > 10$, which is already sufficient information to evaluate the scalar mass contribution (3.12) to a reasonable accuracy.

### *5.3. Scalar partner masses*

Once we have determined the values of $m_2$ and tan $\beta$ and have either verified gaugino universality or measured the independent gaugino masses, we are ready to measure the masses of squarks and sleptons that will contribute to the Dine-Nelson plot. From the various spectra shown in Fig. 4, it is likely that the sleptons can be found at least at a 1 TeV linear collider, and it is possible that the squarks could also be found at such a facility.

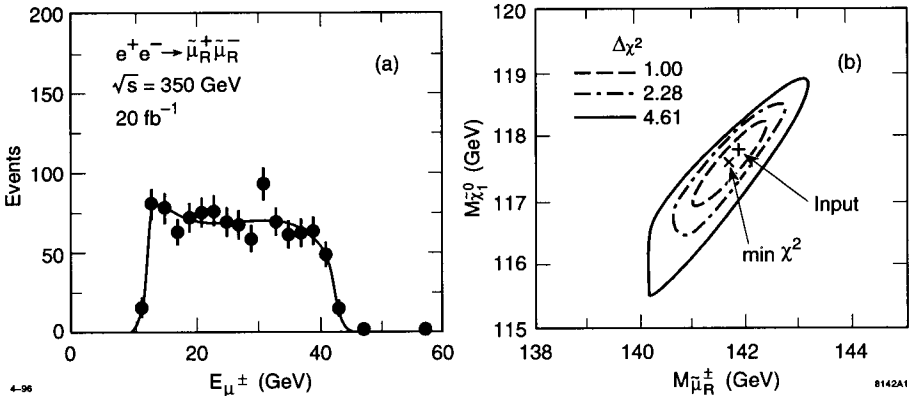


Fig. 15. Determination of the $\tilde{\mu}_R$ mass in the decay $\tilde{\mu}_R^- \to \mu^-\tilde{\chi}_1^0$, according to the simulation results of Ref. 25. The analysis assumes right-handed electron polarization $P$ = 0.95. The right-hand figure shows the $\chi^2$ distribution as a function of the masses of $\tilde{\mu}_R^-$ and $\tilde{\chi}_1^0$.

Consider first the sleptons. The simplest possible decay of a slepton is

$$\tilde{\ell}^- \to \ell^-\tilde{\chi}_1^0 , \tag{5·29}$$

and this mode has a substantial branching ratio thorough most of the parameter space. This leads to events of the form $e^+e^- \to \ell^+\ell^-\tilde{\chi}_1^0\tilde{\chi}_1^0$ which are very simple to analyze.

The only important background to these events comes from $e^+e^- \to W^+W^-$, and this can be reduced by using a polarized $e^-_R$ beam. The lepton energy distribution from the decay of the scalar $\tilde{\ell}$ is flat, with a sharp cutoff at the kinematic endpoints. By fitting the endpoints, one determines the mass of the parent $\tilde{\ell}$ and the mass of the $\tilde{\chi}^0_1$ into which it decays. Simulation results on the determination of the $\tilde{\mu}$ mass, taken from Ref. 25, are shown in Fig. 15. This analysis corresponds to a 1% mass determination for the slepton and for the lightest neutralino. The superpartners of left- and right-handed leptons can be distinguished by their $SU(2)\times U(1)$ quantum numbers as determined from the values of their production cross sections and polarization asymmetries. Thus, for the sleptons, we can expect to obtain very accurate measurements to fill in the pattern on the left-hand side of the Dine-Nelson plot.

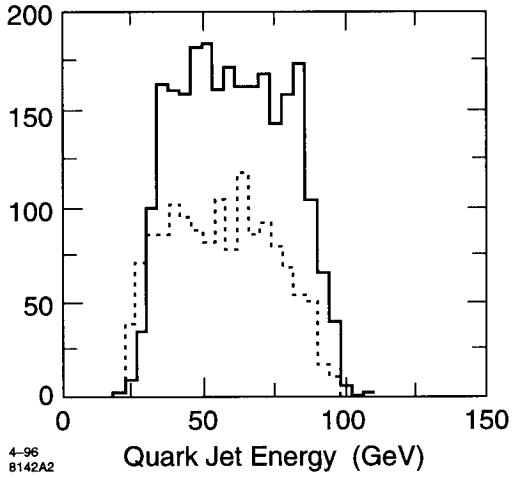


Fig. 16. Distribution of quark jet energies in squark decay in one region of parameter space studied in Ref. 52. The solid (dashed) histogram refers to events with $e^-_L(e^-_R)$ polarized beams.

If squarks lie above the energy range of the linear collider, we must be content with the 10–1570 measurement of the average squark mass that will emerge from the analysis of supersymmetry observable at the LHC. However, if the linear collider can produce squarks, some more elegant experiments are possible. For example, $e^+e^-$ annihilation with an $e^-_L$ beam dominantly produces the superpartners of left-handed quarks, while the use of an $e^-_R$ beam dominantly produces the superpartners of right-handed quarks. Feng and Finnell[52] have shown that it is possible to use this asymmetry to measure the mass difference between $\tilde{q}_L$ and $\tilde{u}_R, d_R$. Consider, for example, the particularly favorable region in which all species of squarks decay dominantly to $q\tilde{\chi}^0_1$. A simulation of the distribution of quark jet energies from squark production, for a particular point in this region, is shown in Fig. 16. As with the lepton energy distribution in slepton decay, the quark energy distribution is flat and cuts off sharply at the endpoint. By comparing the location of the endpoint for the two electron beam polarizations, it is possible to measure the left-right squark mass difference to 1% of the squark mass. Using more sophisticated techniques described in Ref. 52, it is possible to reach comparable precision in other regions of the parameter space.

One interesting unsolved problem is the question of how to measure the $\tilde{u}_R$–$\tilde{d}_R$

mass difference. With this quantity under control, the full pattern on the Dine-Nelson plot would be revealed experimentally. However, you can see from Fig. 4 that the precision flavor- and helicity-selected measurement of slepton masses, plus a reasonable knowledge of the average squark mass, already distinguishes the various classes of models shown. This information can realistically be made available by combining the results of LHC and linear collider experiments.

## §6. Conclusion

In this article, I have tried to sketch out the experimental program that would follow from the discovery of supersymmetry at the weak interaction scale. It is an important question whether supersymmetry is present at the TeV scale, and whether it is the mechanism of electroweak symmetry breaking. But, if indeed Nature chooses this mechanism, what we have to learn at the next generation of colliders goes far beyond this single piece of information. The spectrum of supersymmetric particles contains information which bears directly on the physics of very short distances, perhaps even down to the unification or gravitational scale. The challenge will be to extract this information and study its lessons.

Pursuing this goal, I have set out a three-step program to clarify the physics of the supersymmetry mass spectrum. To set the scale of superpartner masses, we first need to measure the gaugino masses and the Higgs sector parameter $\tan\beta$. In the process, we must test the hypothesis of gaugino universality. Then, incorporating all of this information, we can measure the slepton and squark masses and try to recognize their pattern as characteristic of a specific messenger of supersymmetry breaking.

Electron-positron colliders have a major role to play in this program. Using their access to the simplest supersymmetry reactions and the control of beam polarization, these facilities allow model-independent measurements of the uncolored gaugino masses. They can also provide accurate, helicity-specific measurements of the slepton masses. If the squarks are sufficiently light, linear colliders can be used to measure the helicity-specific squark masses as well.

Hadron collider experiments can be expected to pin down the masses of the heavier states of supersymmetry, the squarks and gluinos. However, the observable which are useful for hadron experiments require for their interpretation a detailed model of the decay pattern of strongly-interacting superpartners. Thus, the interpretation of experimental results from hadron collider will also rely on the precision information available from $e^+e^-$ colldiers.

It is daunting that the detailed study of supersymmetry will require a number of new and expensive experimental facilities. But we can already anticipate that these facilities will suffice to give us concrete information on the spectrum of superpartners, information we can use to determine the mechanism of supersymmetry breaking and the linkage of weak-scale supersymmetry to deep theoretical speculations. It is a pleasant dream that in the future we might have direct experimental information on the physics of the unification or the superstring scale. With these new tools—the LHC and the $e^+e^-$ linear collider—we can make this dream a reality.

**Acknowledgements**

The ideas expressed here have been strongly influenced by discussions with Howard Baer, Tim Barklow, Michael Dine, Savas Dimopoulos, Lance Dixon, Keisuke Fujii, Howard Haber, Jonathan Feng, Gordon Kane, Hitoshi Murayama, and Xerxes Tata. I am grateful to them, and to many other colleagues at SLAC and in the broader community, for educating me in this area. I am deeply grateful to Taichiro Kugo and the organizers of the YKIS '95 meeting for their hospitality in Kyoto. This work was supported by the Department of Energy under contract DE–AC03–76SF00515.

References

1) P. Langacker and N. Polonsky, Phys. Rev. **D47** (1993) 4028, Phys. Rev. **D52** (1995) 3081.
2) L. E. Ibáñez and G. G. Ross, in *Perspectives on Higgs Physics*, G. L. Kane, ed. (World Scientific, Singapore, 1993).
3) H. P. Nines, Phys. Repts. **110** (1984) 1.
4) H. E. Haber and G. L. Kane, Phys. Repts. **117** (1985) 75.
5) S. Dimopoulos, in *Proceedings of the XXVII International Conference on High Energy Physics*, vol. 1, P. J. Bussey and I. G. Knowles, eds. (Institute of Physics, Bristol, 1995).
6) H. Murayama and M. E. Peskin, preprint SLAC-PUB-7149, to appear in Ann. Rev. Nucl. Sci.
7) J. Ellis, K. Enqvist, D. V. Nanopoulos, and F. Zwirner, Mod. Phys. Lett. **A1** (1986) 57; R. Barbieri and G. F. Giudice, Nucl. Phys. **B306** (1988) 63; G. G. Ross and R. G. Roberts, Nucl. Phys. **B377** (1992) 571; G. W. Anderson and D. J. Castaño, Phys. Rev. **D52** (1995) 1693, preprint hep-ph/9509212.
8) S. Dimopoulos and L. Hall, Phys. Lett. **B207** (1988) 210; H. Dreiner and G. G. Ross, Nucl. Phys. **B365** (1991) 597.
9) V. S. Kaplunovsky and J. Louis, Phys. Lett. **B306** (1993) 269.
10) A. Brignole, L. E. Ibanez, and C. Munoz, Nucl. Phys. **B422** (1994) 125, E **B436** (1995) 747.
11) E. Witten, Mod. Phys. Lett **A10** (1995) 2153.
12) E. Cremmer, B. Julia, J. Scherk, S. Ferrara, L. Girardello, and P. van Nieuwenhuizen, Nucl. Phys. **B147** (1979) 105; E. Cremmer, S. Ferrara, L. Girardello, and A. Van Proeyen, Nucl. Phys. **B212** (1983) 413.
13) F. Gabbiani and A. Masiero, Nucl. Phys. **B322** (1989) 235.
14) J. S. Hagelin, S. Kelley, and T. Tanaka, Nucl. Phys. **B415** (1994) 293; S. Dimpoulos and D. Sutter, Nucl. Phys. **B452** (1995) 496; E. Gabrielli, A. Masiero, L. Silvestrini, preprints hep-ph/9509379, hep-ph/9510215.
15) S. Dimopoulos and H. Georgi, Nucl. Phys. **B193** (1981) 150.
16) N. Sakai, Z. Phys. **C11** (1981) 153.
17) A. H. Chamseddine, R. Arnowitt, and P. Nath, Phys. Rev. Lett. **49** (1982) 970, Nucl. Phys. **B227** (1983) 1219; "R. Barbieri, S. Ferrara, and C. A. Savoy, Phys. Lett. **B119** 1982) 343; L. Hall, J. Lykken, and S. Weinberg, Phys. Rev. **D27** (1983) 235.
18) J. Ellis, C. Kounnas, and D. V. Nanopoulos, Nucl. Phys. **B247** (1984) 373.
19) M. Lanzagorta and G. G. Ross, Phys. Lett. **B349** (1995) 319, Phys. Lett. **B364** 1995) 163.
20) M. Dine, A. E. Nelson, and Y. Shirman, Phys. Rev. **D51** (1995) 1362; M. Dine, A E. Nelson, Y. Nir, and Y. Shirman, preprint hep-ph/9507378.
21) M Leurer, Y. Nir, and N. Seiberg, Nucl. Phys. **B420** (1994) 468.
22) S. Dimopoulos. G. F. Giudice. and N. Tetradis, Phys. Lett. **B357** (1995) 573.
23) I. Jack and D. R. T. Jones, Phys. Lett. **B333** (1994) 372; S. P. Martin and M. T. Vaughn, Phys. Rev. **D50** (1994) 2282; Y. Yamada, Phys. Rev. **D50** (1994) 3537; I. Jack, *et al.*, Phys. Rev. **D50** (1994) 5481.
24) S. P. Martin and M. T. Vaughn, Phys. Lett. **B318** (1993) 331; D. Pierce and A. Papadopoulos, Nucl. Phys. **B430** (1994) 278.

25) T. Tsukamoto, K. Fujii, H. Murayama, M. Yamaguchi, and Y. Okada, Phys. Rev. **D51** (1995) 3153.
26) J. L. Feng, N. Polonsky, and S. Thomas, preprint hep-ph/951 1324.
27) A. Kusenko, P. Langacker, and G. Segre, preprint hepph/9602414.
28) H. C. Cheng and L. Hall, Phys. Rev. **D51** (1995) 5289.
29) Y. Kawamura, H. Murayama, and M. Yamaguchi, Phys. Rev. **D51** (1995) 1337.
30) C. Kolda and S. P. Martin, preprint hep-ph/9503445.
31) J. Lopez and D. V. Nanopoulos, preprint hep-ph/9412332.
32) K. Choi, preprint hep-ph/9509430.
33) R. Barbieri and L. J. Hall, Phys. Lett. **B338** (1994) 212; R. Barbieri, L. J. Hall, and A. Strumia, Nucl. Phys. **B445** (1995) 219.
34) N. Arkani-Hamed, H.-C. Cheng, J. L. Feng, and L. J. Hall, preprint hep-ph/9603431.
35) D. R. Stump, M. Wiest, and C.-P. Yuan, preprint hep-ph/9601362.
36) S. Dimopoulos, M. Dine, S. Raby, and S. Thomas, preprint hep-ph/9601367.
37) J. L. Feng and M. J. Strassler, Phys. Rev. **D51** (1995) 4661.
38) B. de Carlos and M. A. Diaz, preprint hep-ph/9511421.
39) CMS Collaboration, Technical Proposal. CERN/LHCC/94-38 (1994).
40) ATLAS Collaboration, Technical Proposal. CERN/LHCC/94-43 (1994).
41) H. Baer, X. Tata, and J. Woodside, Phys. Rev. **D45** (1992) 142.
42) H. Baer, V. Barger, D. Karatas, and X. Tata, Phys. Rev. **D36** (1987) 96; R. M. Barnett, J. F. Gunion, and H. E. Haber, Phys. Rev. **D37** (1988) 1892; H. Baer, X. Tata, and J. Woodside, Phys. Rev. **D42** (1990) 1568.
43) H. Baer, C.-H. Chen, F. Paige, and X. Tata, Phys. Rev. **D49** (1994) 3283, preprint hep-ph/9512383.
44) J. L. Lopez, D. V. Nanopoulos, X. Wang, and A. Zichichi, Phys. Rev. **D48** (1993) 2062; H. Baer, C. Kao, and X. Tata, Phys. Rev. **D48** (1993) 5175.
45) H. Baer, C.-H. Chen, F. Paige, and X. Tata, Phys. Rev. **D50** (1994) 4508.
46) R. M. Barnett, J. F. Gunion, and H. E. Haber, Phys. Lett. **B315** (1993) 349.
47) H. Baer, C.-H. Chen, F. Paige, and X. Tata, Phys. Rev. **D52** (1995) 2746.
48) S. Basa, Marseille Ph. D. thesis, 1994.
49) H. Baer, A. Bartl, D. Karatas, W. Majerotto, and X. Tata, Intl. J. Mod. Phys. **A4** (1989) 4111.
50) J. L. Feng, M. E. Peskin, H. Murayama, and X. Tata, Phys. Rev. **D52** (1995) 1418.
51) M. M. Nojiri, Phys. Rev. **D51** (1995) 6281.
52) J. L. Feng and D. E. Finnell, Phys. Rev. **D49** (1994) 2369.